

In the format provided by the authors and unedited.

# Catalytic transport of molecular cargo using diffusive binding along a polymer track

Lifei Zheng<sup>1,8\*</sup>, Hui Zhao<sup>1,2,8</sup>, Yanxiao Han<sup>3,8</sup>, Haibin Qian<sup>1</sup>, Lela Vukovic<sup>4</sup>, Jasmin Mecinović<sup>1,7</sup>, Petr Král<sup>3,5,6</sup> and Wilhelm T. S. Huck<sup>1\*</sup>

---

<sup>1</sup>Radboud University, Institute for Molecules and Materials, Nijmegen, The Netherlands. <sup>2</sup>Institute of Fundamental and Frontier Sciences (IFFS), University of Electronic Science and Technology of China (UESTC), Chengdu, China. <sup>3</sup>Department of Chemistry, University of Illinois at Chicago, Chicago, IL, USA. <sup>4</sup>Department of Chemistry and Biochemistry, University of Texas at El Paso, El Paso, TX, USA. <sup>5</sup>Department of Physics, University of Illinois at Chicago, Chicago, IL, USA. <sup>6</sup>Department of Biopharmaceutical Sciences, University of Illinois at Chicago, Chicago, IL, USA. <sup>7</sup>Present address: Department of Physics, Chemistry and Pharmacy, University of Southern Denmark, Campusvej 55, Odense, Denmark. <sup>8</sup>These authors contributed equally: Lifei Zheng, Hui Zhao and Yanxiao Han. \*e-mail: [zhenglifei0926@gmail.com](mailto:zhenglifei0926@gmail.com); [w.huck@science.ru.nl](mailto:w.huck@science.ru.nl)

## Table of contents

<b>1. General.....</b>	<b>3</b>
<b>2. Isothermal Titration Calorimetry (ITC) Analyses.....</b>	<b>3</b>
<b>3. Kinetic studies for fluorogenic reactions.....</b>	<b>8</b>
<b>4. Molecular Dynamic Simulations.....</b>	<b>29</b>
<b>5. Inter-track molecular cargo transport.....</b>	<b>36</b>
<b>6. Molecular cargo transport within physically separated compartments....</b>	<b>46</b>
<b>7. References.....</b>	<b>50</b>

## 1. General

### 1.1. Materials

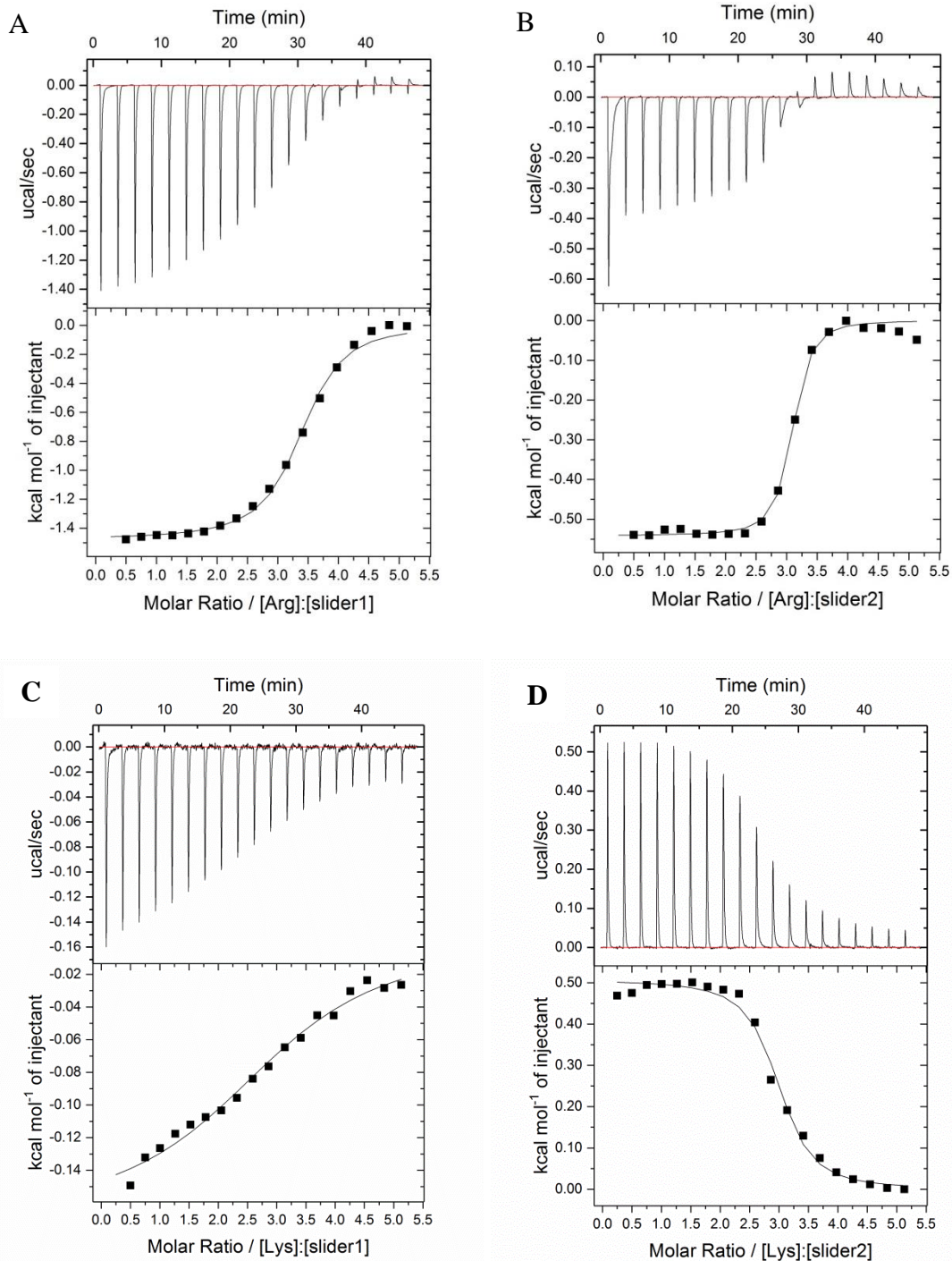
Peptides (>95% purity) were purchased from CASLO ApS (Denmark) and used without further purification. All other chemicals and reagents were used as received from commercial suppliers (e.g. Acros, Sigma Aldrich, Ellsworth, Life Technologies, Lumiprobe) without any further treatment unless stated otherwise. Solvents dimethylformamide (DMF), dimethoxyethane (DME) and dichloromethane ( $\text{CH}_2\text{Cl}_2$ ) for synthesis were distilled prior to use by using molecular sieves (4 Å), metallic sodium and calcium hydride ( $\text{CaH}_2$ ), respectively. For all experiments, ultrapure water (18.2 M $\Omega$ ) purified by a MilliQ-Millipore system was used.

### 1.2. Methods

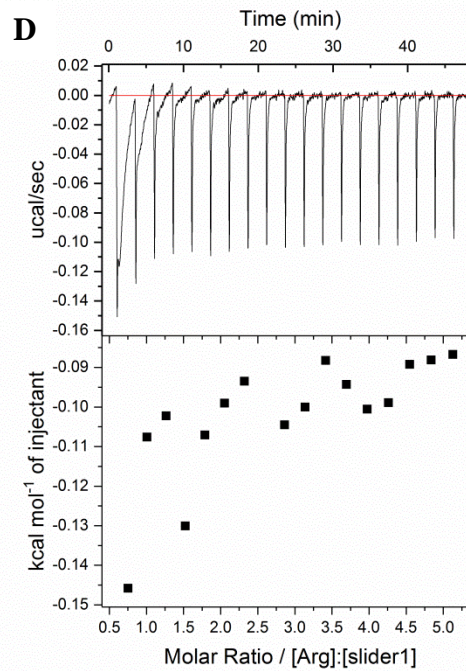
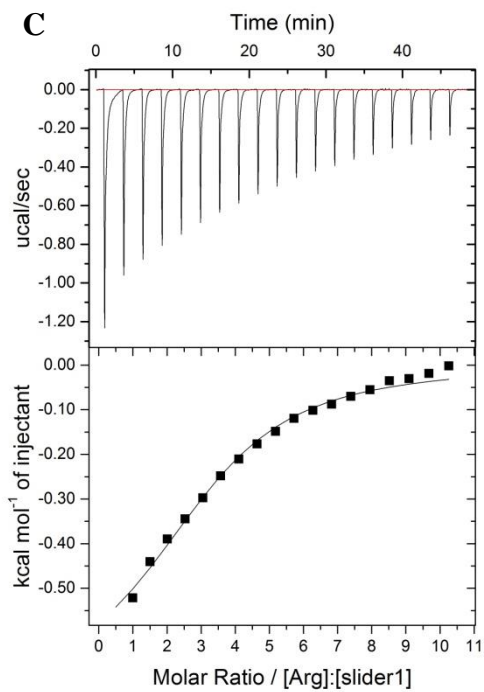
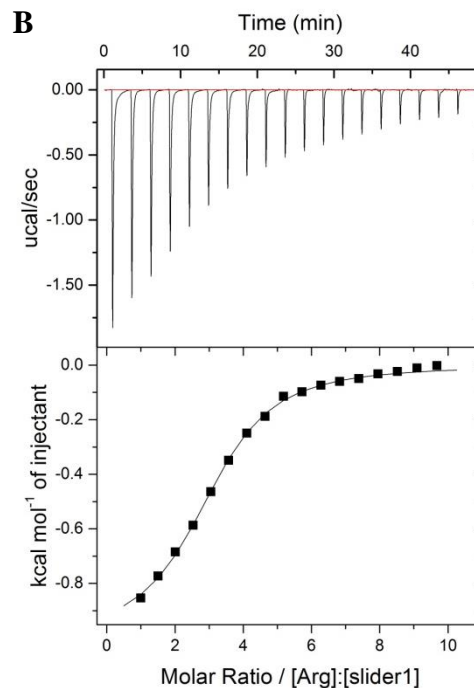
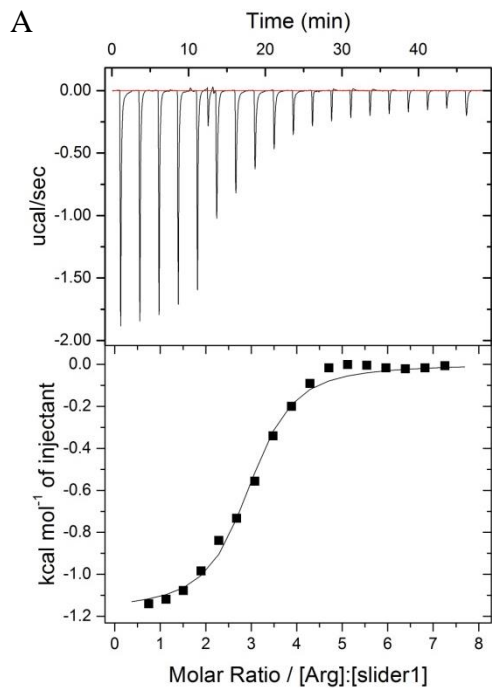
NMR spectra were measured on a Varian INOVA A-400 spectrometer at 400 MHz. The chemical shifts for  $^1\text{H}$  are given in parts per million (ppm) relative to TMS. Mass spectra of small molecules were obtained from Thermo scientific advantage LCQ and JEOL Accurate Time of Flight (TOF) instruments, both using linear ion trap electrospray ionization (ESI). Mass spectrometry of the monodispersed polyArginines were performed using Bruker Microflex LRF MALDI-TOF system with  $\alpha$ -Cyano-4-hydroxycinnamic acid as matrix. Isothermal calorimetry (ITC) measurements were carried out at 25°C with a MicroCal Auto-ITC200. Fluorescence spectra were performed on a Perkin Elmer LS55 fluorescence spectrometer. Kinetic measurements of the fluorogenic reactions were recorded on an Infinite M200 PRO plate reader. A Shimadzu LC-20A Prominence system was used to analyze and purify synthetic Glutamic acid featured oligo- peptides. Diffusion of fluorescently labeled track or slider in gel matrix was recorded on a confocal laser scanning microscope (CLSM) (SP8x, Leica)

## 2. Isothermal Titration Calorimetry (ITC) analyses

In the earlier work <sup>1</sup>, it was pointed out that one set of sites model cannot entirely describe the complicated curves obtained during interactions involving polyelectrolyte complexes. Therefore, our fitting was solely based on the sigmoidal parts of the binding enthalpy curve. Hence, the entropy and enthalpy values were calculated with less accuracy but still comparable, since the heat effect in all titrations were intrinsically small. Most importantly, the obtained binding affinities which we were mostly interested in should be highly reliable, as these were calculated from the slope of the sigmoidal curves.



**Figure 1.** ITC of A) pArg (5 mM in 50 mM MES buffer pH 6.1) into slider 1 (0.2 mM in 50 mM MES buffer pH 6.1); B) pArg (5 mM in 50 mM MOPS buffer pH 7.1) into slider 2 (0.2 mM in 50 mM MOPS buffer pH 7.1); C) pLys (5 mM in 50 mM MES buffer pH 6.1) into slider 1 (0.2 mM in 50 mM MES buffer pH 6.1); D) pLys (5 mM in 50 mM MOPS buffer pH 7.1) into slider 2 (0.2 mM in 50 mM MOPS buffer pH 7.1).



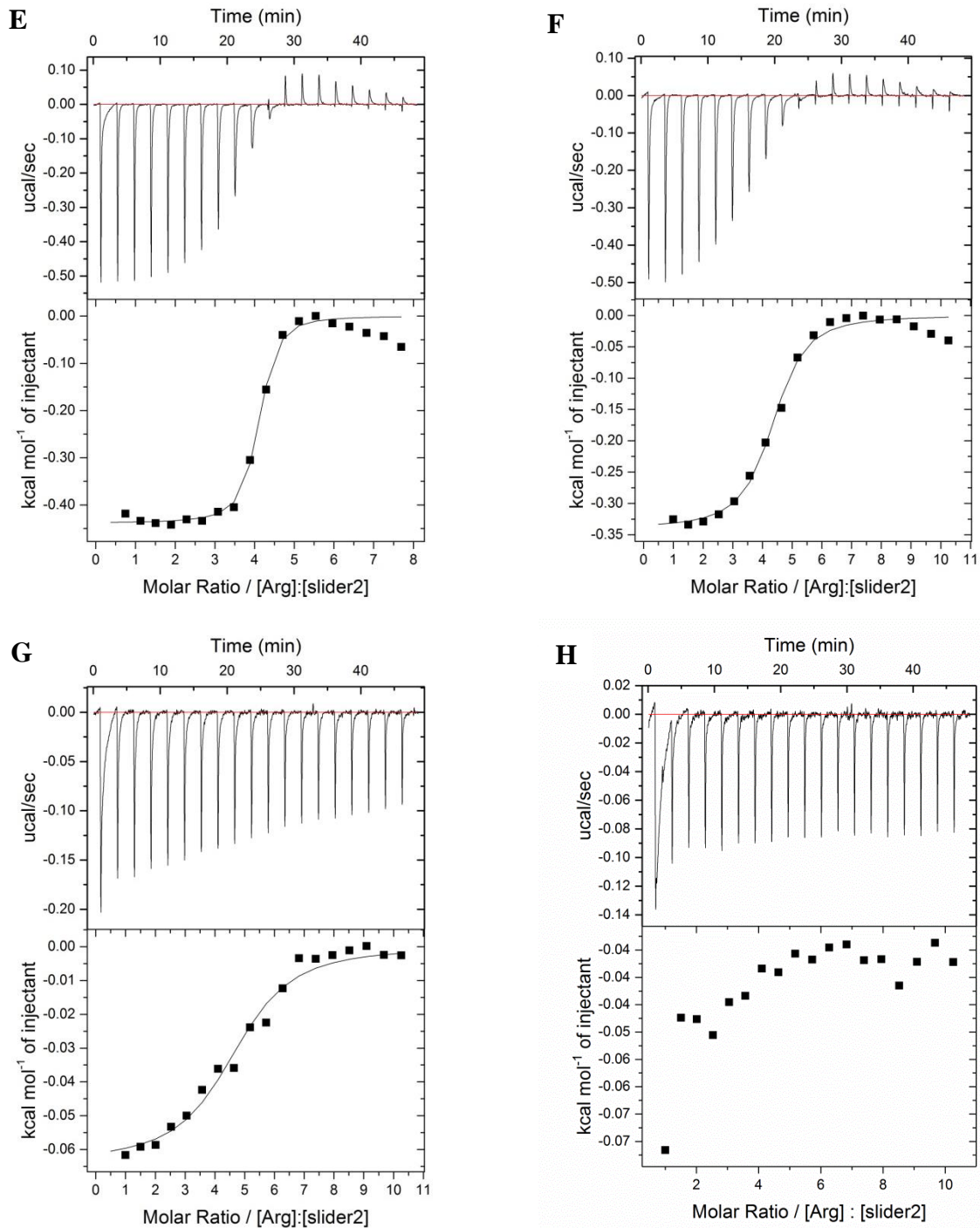


**Figure 2.** ITC of A) pArg (7.5 mM in 50 mM MES buffer containing 50 mM NaCl) into slider 1 (0.2 mM in 50 mM MES buffer containing 50 mM NaCl); B) pArg (10 mM in 50 mM MES buffer containing 100 mM NaCl) into slider 1 (0.2 mM in 50 mM MES buffer containing 100 mM NaCl); C) pArg (10 mM in 50 mM MES buffer containing 200 mM NaCl) into slider 1 (0.2 mM in 50 mM MES buffer containing 200 mM NaCl); D) pArg (5 mM in 50 mM MES buffer containing 500 mM NaCl) into slider 1 (0.2 mM in 50 mM MES buffer containing 500 mM NaCl); E) pArg

(10 mM in 50 mM MOPS buffer containing 50 mM NaCl) into slider 2 (0.2 mM in 50 mM MOPS buffer containing 50 mM NaCl); F) pArg (10 mM in 50 mM MOPS buffer containing 100 mM NaCl) into slider 2 (0.2 mM in 50 mM MOPS buffer containing 100 mM NaCl); G) pArg (10 mM in 50 mM MOPS buffer containing 200 mM NaCl) into slider 2 (0.2 mM in 50 mM MOPS buffer containing 200 mM NaCl); H) pArg (10 mM in 50 mM MOPS buffer containing 500 mM NaCl) into slider 2 (0.2 mM in 50 mM MOPS buffer containing 500 mM NaCl).

**Table 1.** The dependence of binding affinity of pArg•slider 1/2 on NaCl concentrations.

pArg • slider 1/2	No NaCl	50 mM NaCl	100 mM NaCl	200 mM NaCl
$K_d$ ( $\mu\text{M}$ )	6.9 / 1.3	16.6 / 2.4	68 / 14	200 / 43
$\Delta H^\circ$ (kcal/mol)	-1.48 / -0.54	-1.17 / -0.44	-0.99 / -0.34	0.74 / 0.06
$T\Delta S^\circ$ (kcal/mol)	5.57 / 7.48	5.36 / 7.21	4.68 / 6.29	4.32 / 5.90

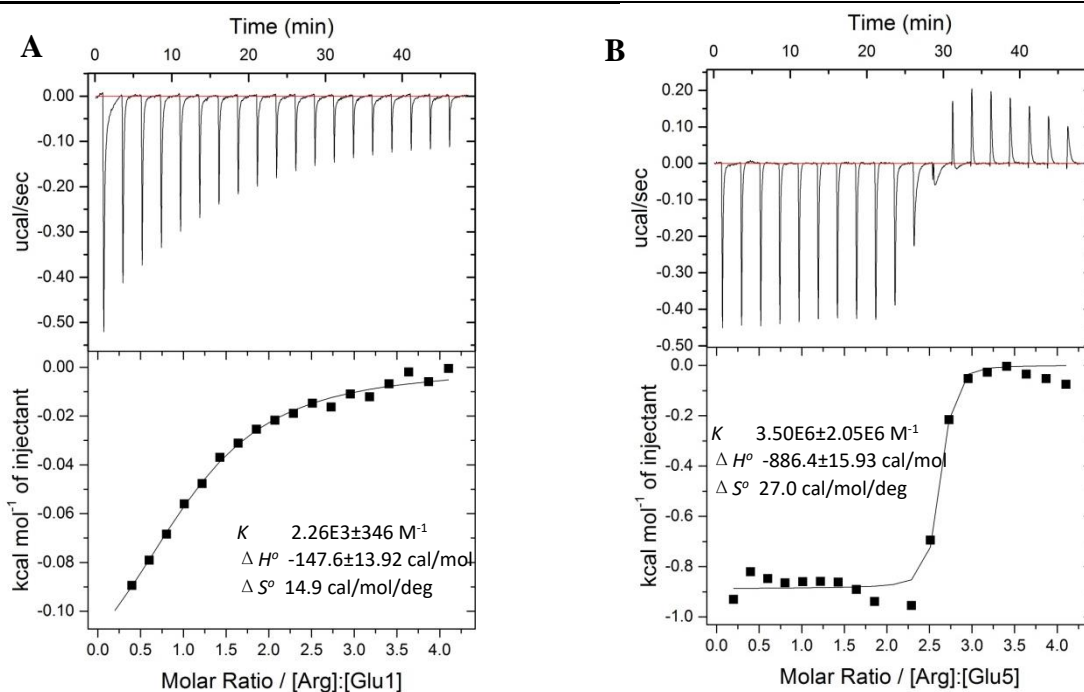


**Figure 3.** ITC of A) pArg (20 mM in 50 mM MOPS buffer pH 7.1) into Glu1 (1 mM in 50 mM MOPS buffer pH 7.1); B) pArg (5 mM in 50 mM MOPS buffer pH 7.1) into Glu5 (0.2 mM in 50 mM MOPS buffer pH 7.1).



### 3. Kinetic studies for fluorogenic reactions

#### 3.1. Synthesis of bromo-substituted N-methyl-maleimide-Acetylcysteamine (**3**)

In a 20mL glass bottle, 3,4-dibromo-1-methyl-1H-pyrrole-2,5-dione (50 mg; 0.18 mmol) was dissolved in 5 mL of methanol. N-acetylcysteamine (21 mg; 0.18 mmol) was added into the reaction mixture. The reaction mixture was stirred for overnight at room temperature. The solvent were removed under reduced pressure, and the crude product was purified by silica column using Chloroform/hexane (v/v = 1:3) as the eluent. Isolated yield = 60%.  $^1\text{H NMR}$  (400MHz,  $\text{CDCl}_3$ ): 6.00 (1H, s), 3.55 (4H, m), 3.07 (3H, s), 2.01 (3H, s). ESI MS m/z: mass calculated for  $\text{C}_9\text{H}_{11}\text{BrN}_2\text{O}_3\text{S}$   $[\text{M}+\text{H}]^+=307.0$ , found 306.9.

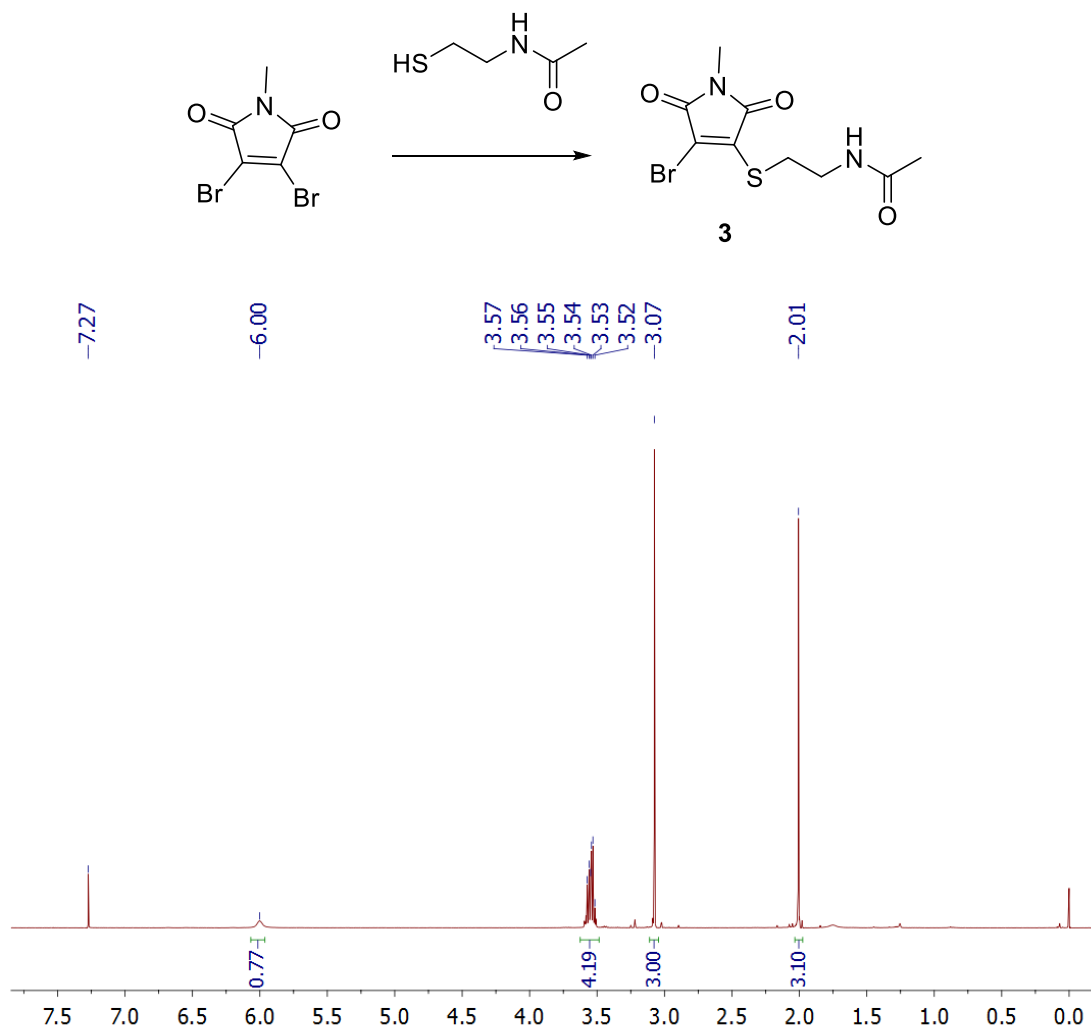
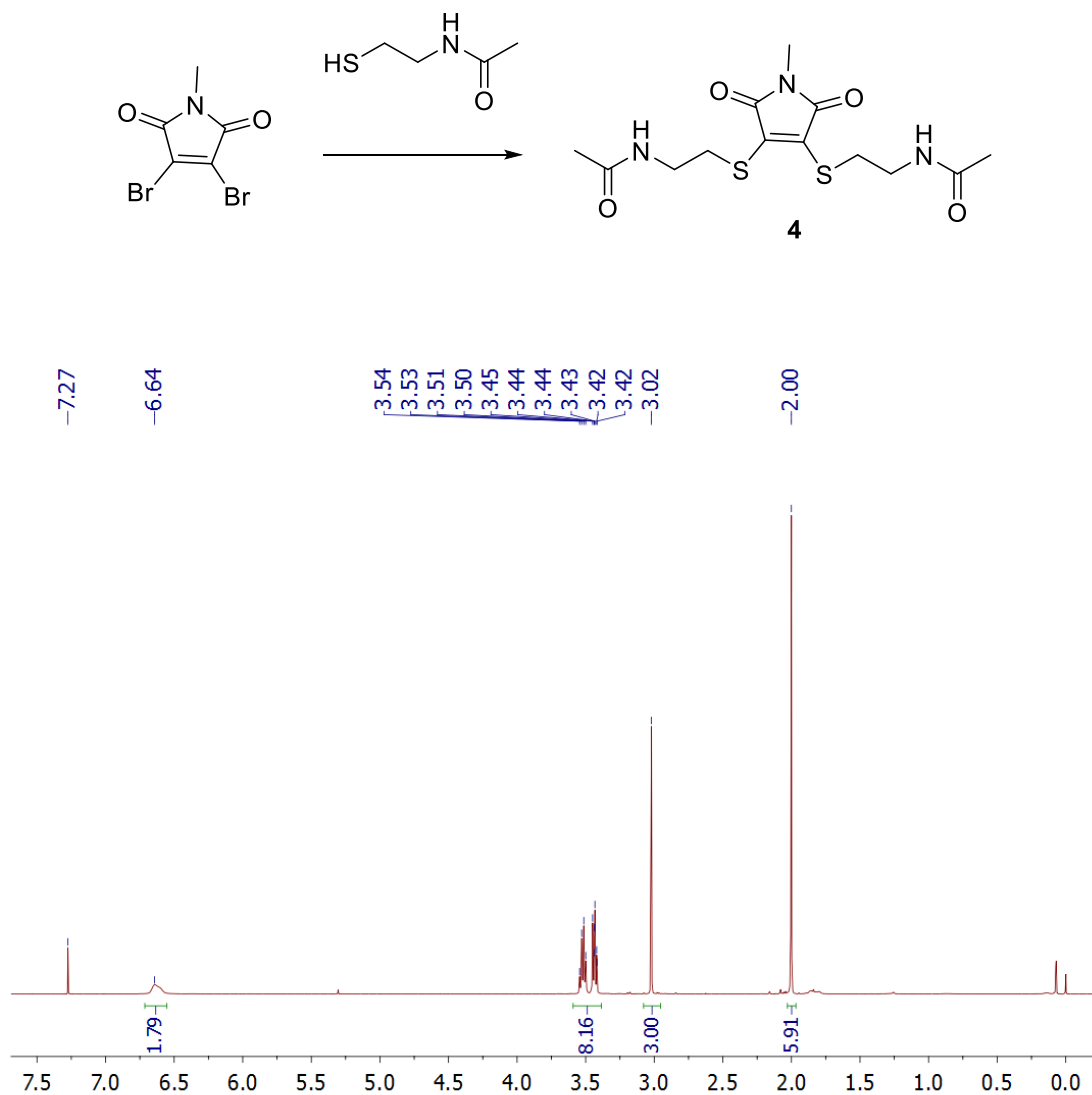


**Figure 4.**  $^1\text{H NMR}$  of compound **3** in  $\text{CDCl}_3$ .

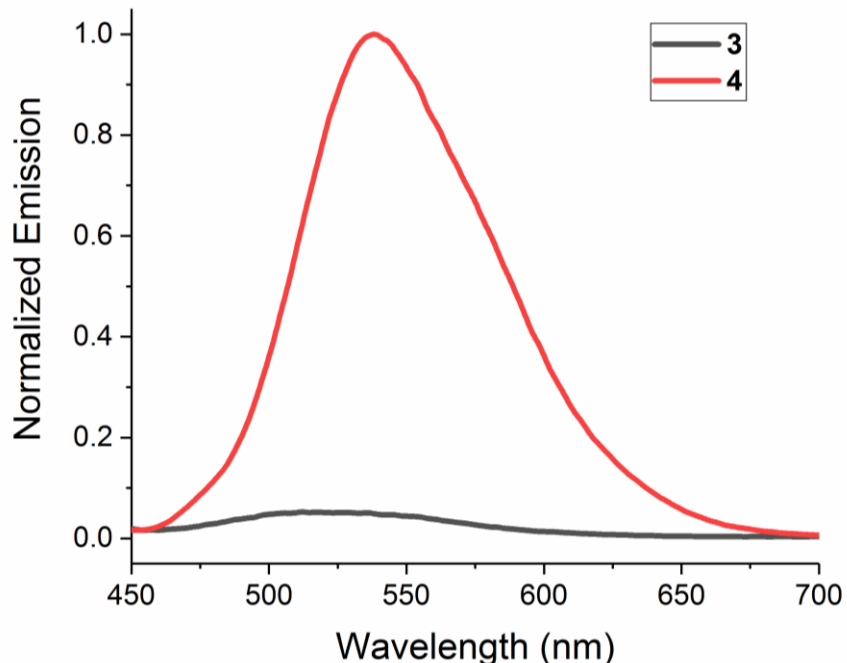


### 3.2. Synthesis of Acetylcysteamine di-substituted N-methyl-maleimide (**4**)

In a 20mL glass bottle, 3,4-dibromo-1-methyl-1H-pyrrole-2,5-dione (50 mg; 0.18 mmol) was dissolved in 5 mL of methanol. N-acetylcysteamine (88 mg; 0.75 mmol) was added into the reaction mixture. The reaction mixture was stirred for overnight at room temperature. The solvent were removed under reduced pressure, and the crude product was purified by silica column using Chloroform/hexane (v/v = 1:3) as the eluent. Isolated yield = 90%.  $^1\text{H NMR}$  (400MHz,  $\text{CDCl}_3$ ): 6.64 (2H, broad), 3.54-3.42 (8H, m), 3.02 (3H, s), 2.00 (6H, s). ESI MS m/z: mass calculated for  $\text{C}_{13}\text{H}_{19}\text{N}_3\text{O}_4\text{S}_2$   $[\text{M}+\text{H}]^+=346.1$ , found 346.0.



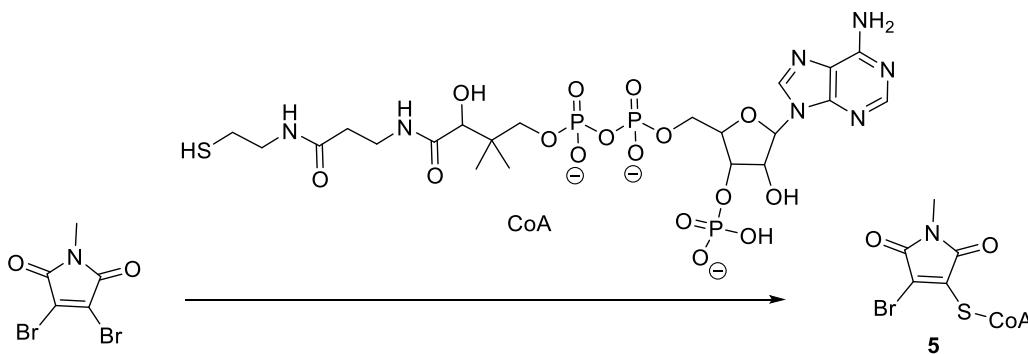
**Figure 5.**  $^1\text{H NMR}$  of compound **4** in  $\text{CDCl}_3$ .



**Figure 6.** Emission spectra of **3** and **4** (0.1 mM in chloroform), measurements were normalized to the higher intensity of **4**. Excitation wavelength: 416 nm.

### 3.3. Synthesis of bromo-substituted N-methyl-maleimide-1 (**5**)

In a 20mL glass bottle, 3,4-dibromo-1-methyl-1H-pyrrole-2,5-dione (188 mg; 0.7 mmol) was dissolved in 2 mL of DMF. Coenzyme A (10 mg; 0.013 mmol) was dissolved in 1 ml of DMF/water (vol/vol=9/1). The CoA solution was added dropwise into the reaction mixture. The reaction mixture was stirred for overnight at room temperature under Argon. The solvent were removed by flushing with N<sub>2</sub>, and the crude product was purified by extraction using E<sub>2</sub>O/water. The final product was obtained after freeze-drying. Isolated yield = 85%. <sup>1</sup>H NMR (400MHz, D<sub>2</sub>O): 8.54 (1H, s), 8.30 (1H, s), 6.07 (1H, d), 4.72 (2H, m), 4.47 (1H, s), 4.13 (2H, s), 3.91 (1H, s), 3.74 (1H, m), 3.49 (1H, m), 3.31 (6H, m), 2.87 (3H, s), 2.31 (2H, t), 0.82 (3H, s), 0.69 (3H, s). ESI MS m/z: mass calculated for C<sub>26</sub>H<sub>38</sub>BrN<sub>8</sub>O<sub>18</sub>P<sub>3</sub>S [M+H]<sup>+</sup>=956.51, found 957.04.



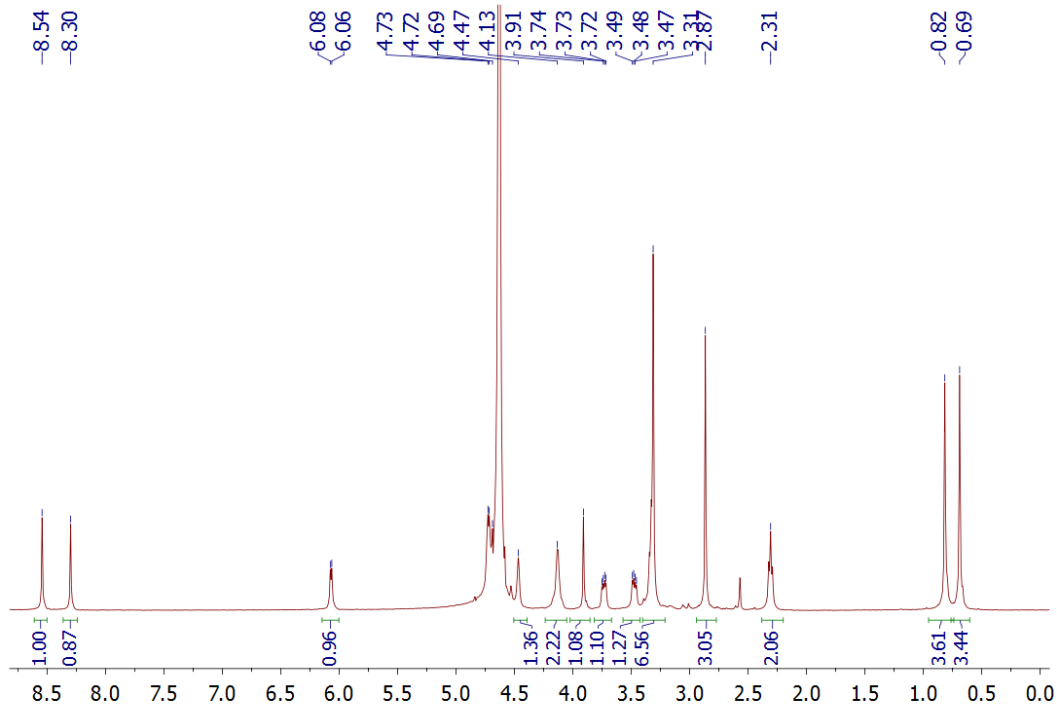


**Figure 7.**  $^1\text{H}$  NMR of compound **5** in  $\text{D}_2\text{O}$ .

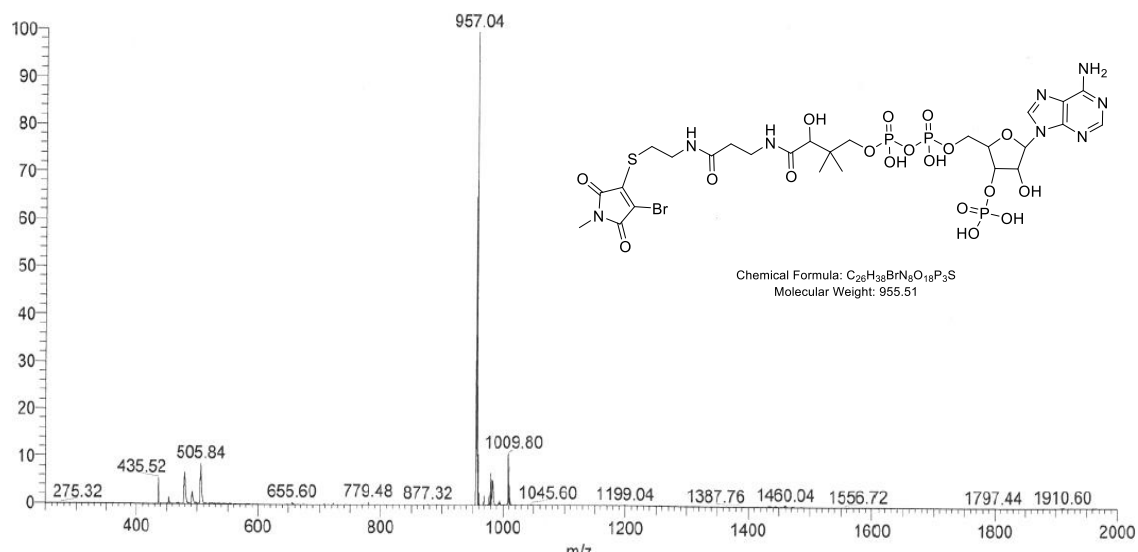


**Figure 8.** ESI-MS analysis of compound **5**.

### 3.4. Synthesis of slider **1** di-substituted N-methyl-maleimide (**6**).

In a 20mL glass bottle, compound 3,4-dibromo-1-methyl-1H-pyrrole-2,5-dione (1.6 mg; 0.006 mmol) was dissolved in 1 mL of water. Coenzyme A (10 mg; 0.013 mmol) was added into the reaction mixture. The reaction mixture was stirred for overnight at room temperature under Argon.

The final product was freeze-dried and obtained with isolated yield of 90%.  $^1\text{H}$  NMR (400MHz,  $\text{D}_2\text{O}$ ): 8.50 (2H, d), 8.26 (2H, d), 6.11-6.01 (2H, m), 4.66 (4H, m), 4.46 (2H, s), 4.13 (4H, m), 3.89 (2H, m), 3.73 (2H, m), 3.50 (2H, m), 3.32-3.12 (12H, m), 2.79 (3H, m), 2.46-2.28 (4H, m), 0.80 (6H, s), 0.67 (6H, s). ESI MS  $m/z$ : mass calculated for  $\text{C}_{47}\text{H}_{73}\text{N}_{15}\text{O}_{34}\text{P}_6\text{S}_2$   $[\text{M}+2\text{H}]^{2+}/2=822.1$ , found 821.0;  $[\text{M}-2\text{H}]^{2-}/2=820.1$ , found 819.2.

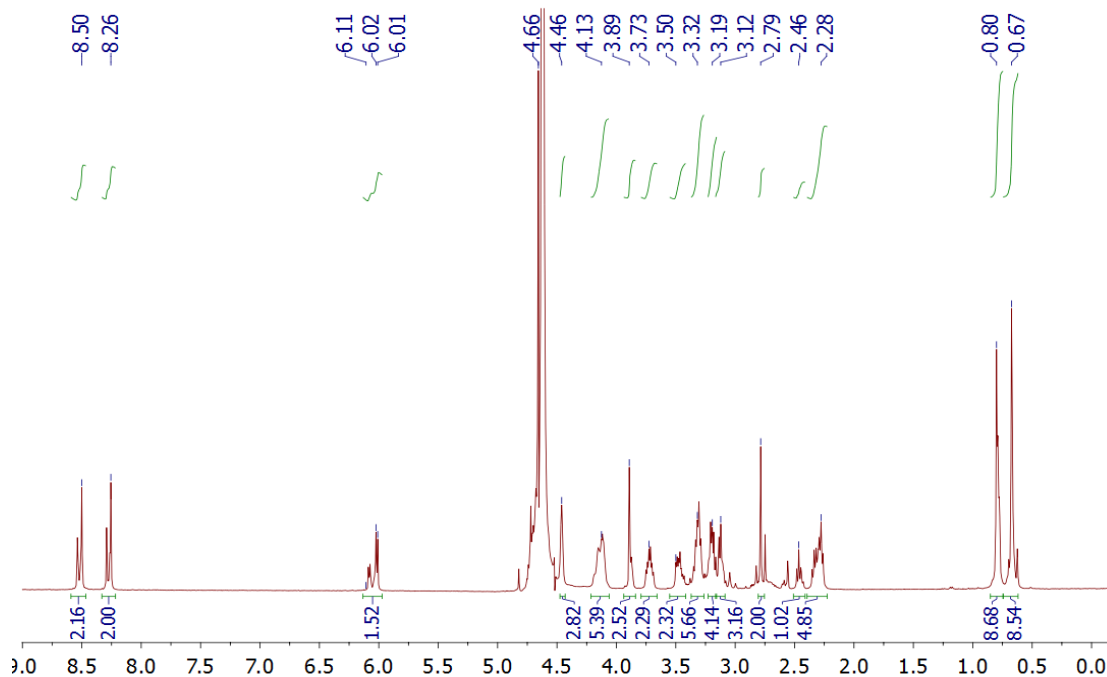
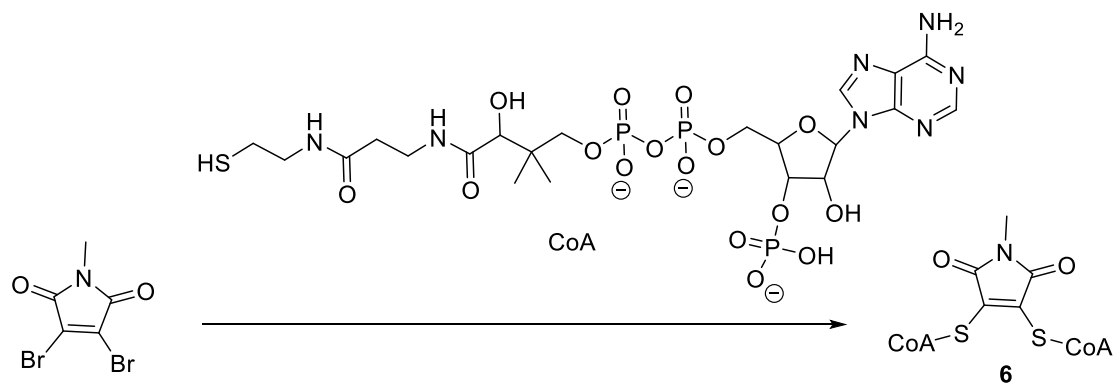


**Figure 9.**  $^1\text{H}$  NMR of compound **6** in  $\text{D}_2\text{O}$ .

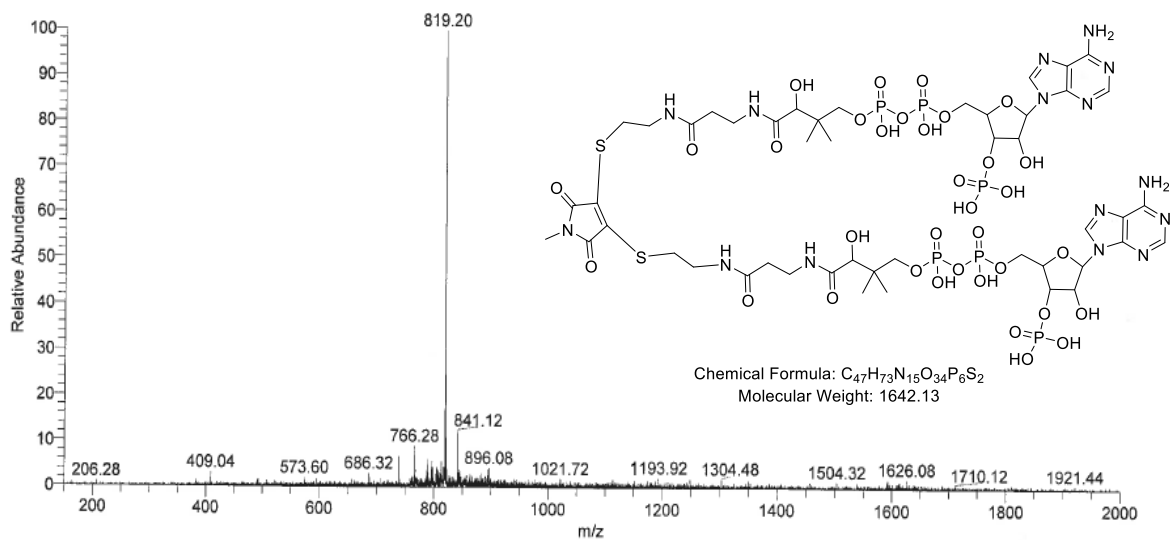


**Figure 10.** ESI-MS analysis of compound **6**, negative charge mode

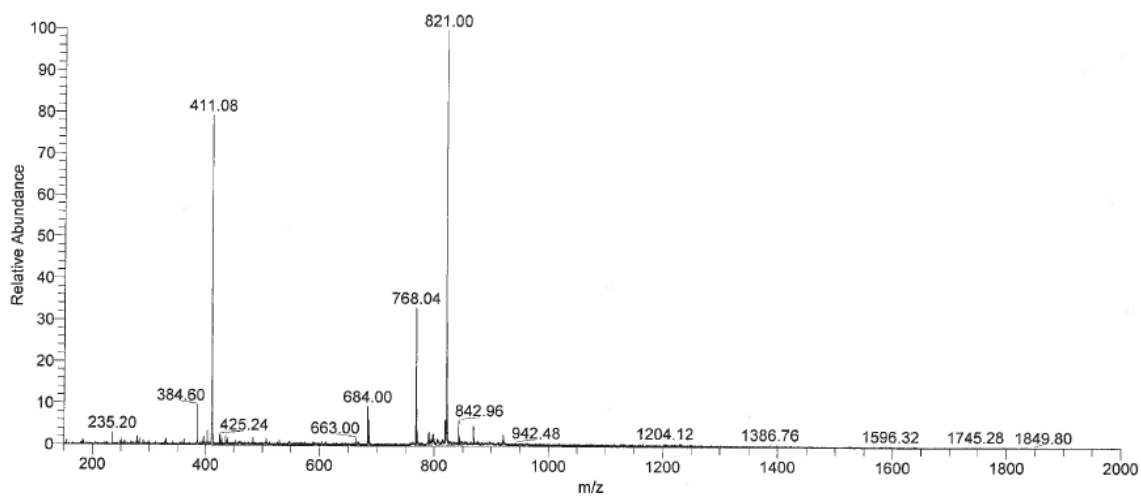


**Figure 11.** ESI-MS analysis of compound **6**, positive charge mode

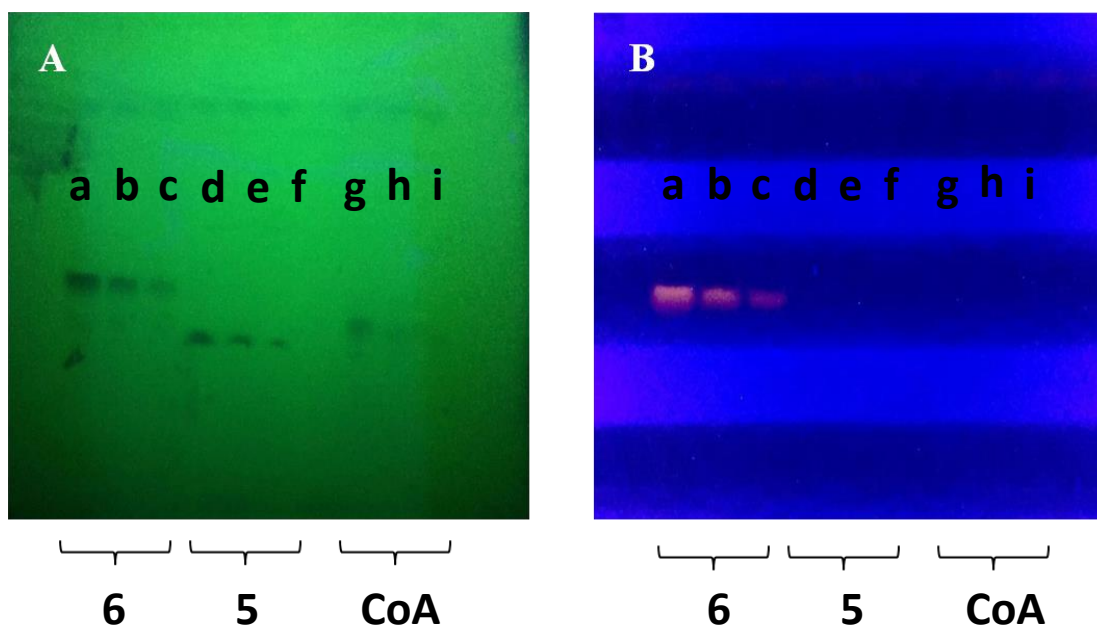


**Figure 12.** Analysis for compound **5** and **6** by denaturing polyacrylamide gel electrophoresis (PAGE) (20 w% in TBE) without subsequent staining. PAGE gel was placed on a silica TLC plate with fluorescent indicator: A) under 254 nm UV light; and B) under 365 nm UV light. Lane a-c: 10 nmol, 1 nmol and 0.1 nmol of compound **6**; Lane d-f: 10 nmol, 1 nmol and 0.1 nmol of compound **5**; Lane g-i: 10 nmol, 1 nmol and 0.1 nmol of CoA.

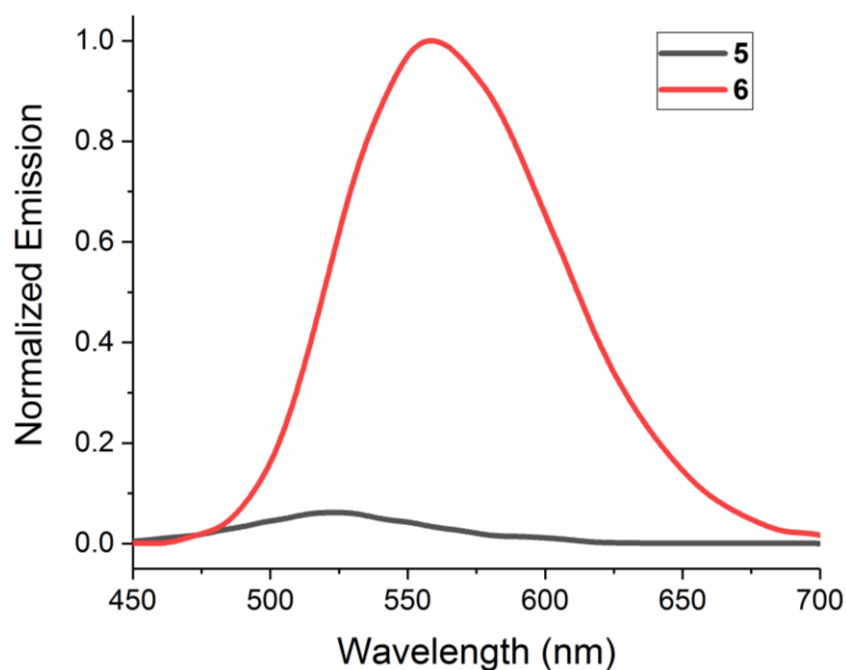
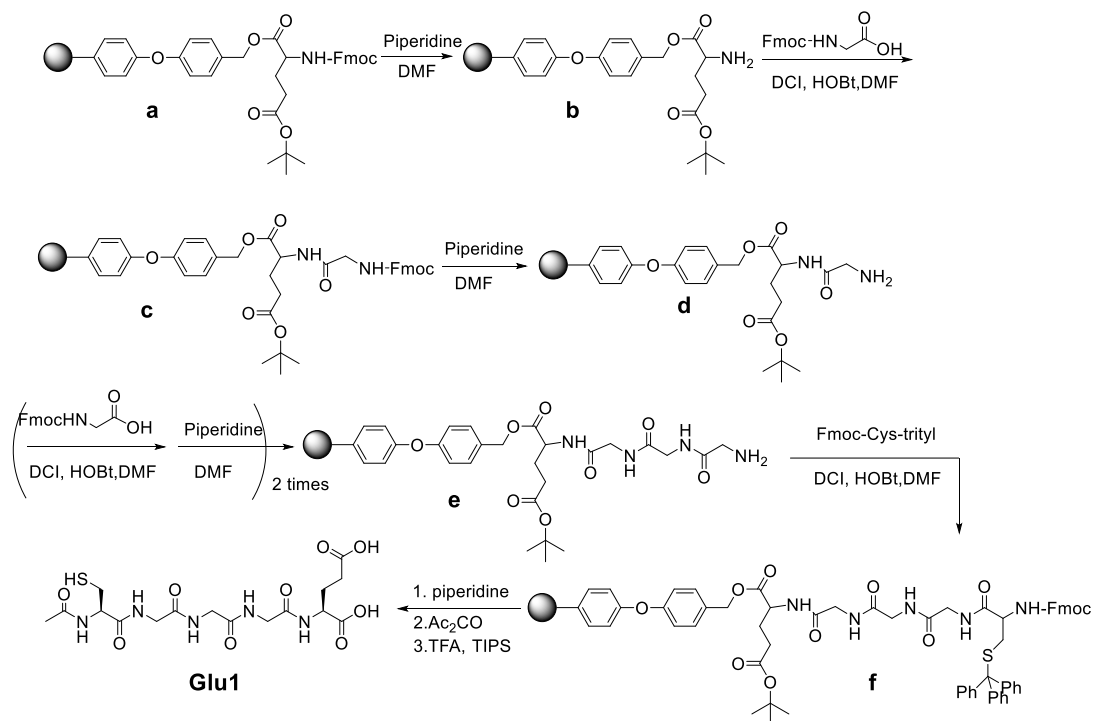


**Figure 13.** Emission spectra of **5** and **6** (0.1 mM in buffer), measurements were normalized to the higher intensity of **6**. Excitation wavelength: 416 nm.

### 3.5. Synthesis of Glu1, Glu3, and Glu5

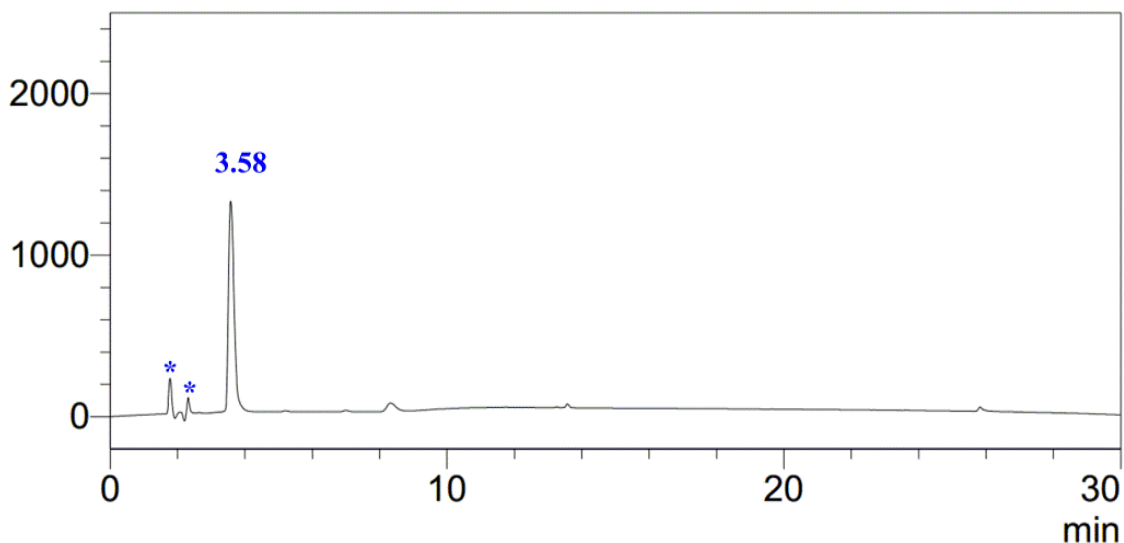


**Scheme 1.** General procedure for the solid phase synthesis of oligopeptides.

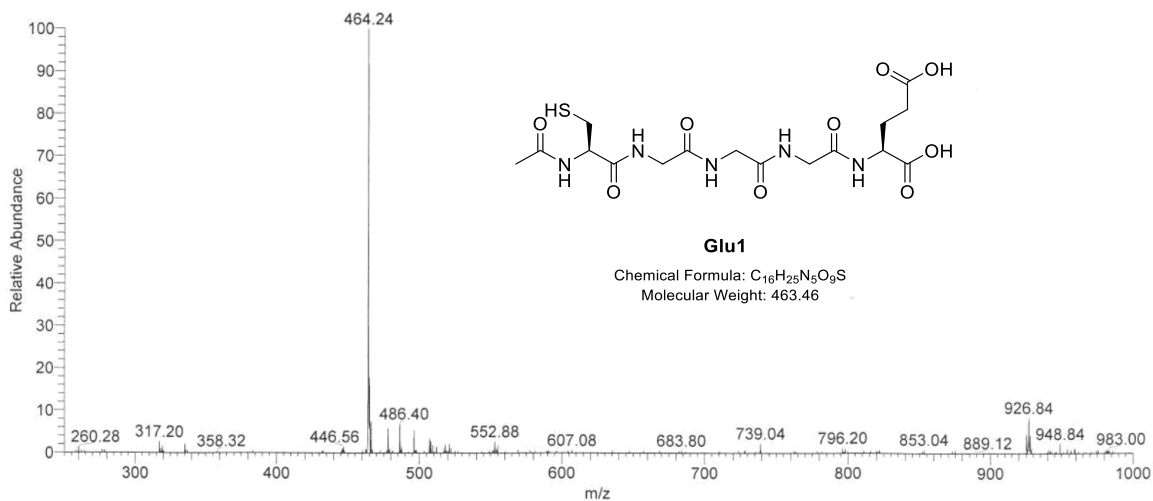
Oligo anion **Glu<sub>n</sub>** (n=1, 3, 5) with free thiols were synthesized using a standard Fmoc solid phase peptide synthesis (SPPS) protocol on Wang resins. Take **Glu1** as example: 2 g Wang resin functionalized with  $\alpha$ -Fmoc-(tBuO)-L-Glutamic acid (0.4 mmol/g) was swollen in DMF for 20 minutes prior to use. Fmoc protecting groups were removed by washing the resin with 15 mL 20% piperidine in DMF, followed by shaking for 20 minutes with another portion of 15 mL piperidine in DMF. Fmoc-Gly-OH (0.9 g, 3 eq.) was coupled to the resin with diisopropylcarbodiimide (DIPCDI, 3.3 eq.) and N-hydroxybenzotriazole (HOBT, 3.6 eq.). Peptide couplings were monitored using Kaiser tests until completion was reached. After coupling, the resin was briefly washed with DMF and subsequently an excess of acetic anhydride and pyridine (>10 eq., 1:1 v/v) was added to the resin. After five minutes, the resin was washed again with DMF to complete a coupling cycle. Then, 2 times of the Fmoc-Gly-OH coupling were carried out. Next, Fmoc-Cys(trityl)-OH were coupled. After the final coupling the remaining Fmoc group was removed and the resin was treated with an excess of acetic anhydride and pyridine (>10 eq., 1:1 v/v). Next, the resin was washed with DMF (3x20 mL), dichloromethane (3x20 mL), methanol (3x20 mL), and again dichloromethane (3x20 mL) before the peptide was cleaved from the resin by applying a mixture of trifluoroacetic acid (TFA)/water/thioanisole (90:5:5, 20 mL) for 8 hours. The peptide was precipitated and washed in diethyl ether (Et2O, 3x80 mL) and air-dried overnight. The crude peptide was purified by preparative HPLC(1%-100% acetonitrile in H2O with 0.1% TFA), affording the final product



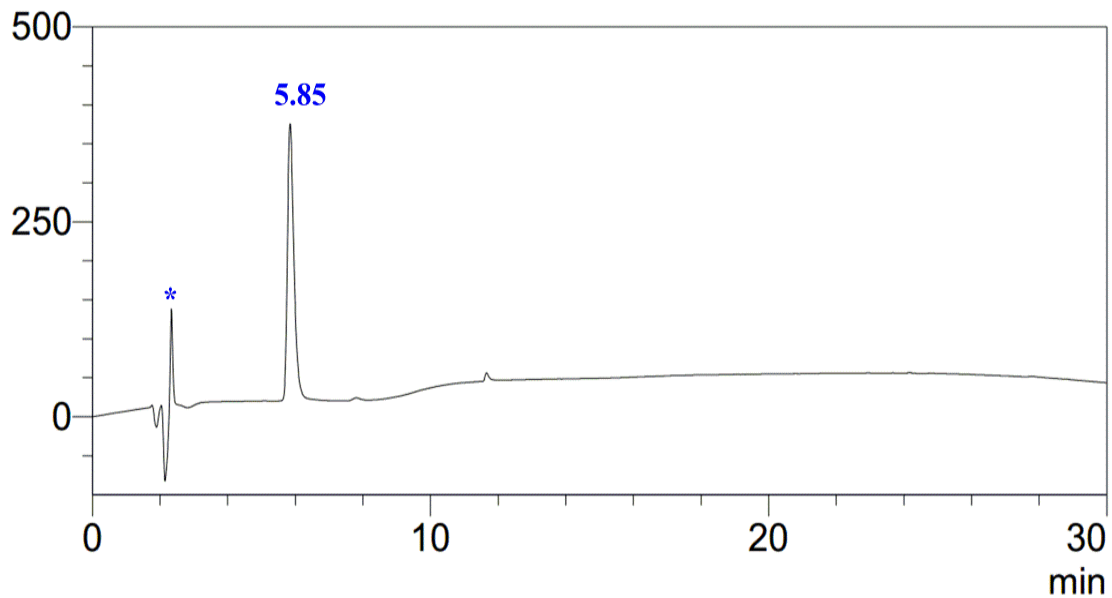
(at retention time 3.58 min) as a white powder after lyophilization. Yield: 50 mg (11%). All the purified peptides were characterized by RP- HPLC and ESI-MS.



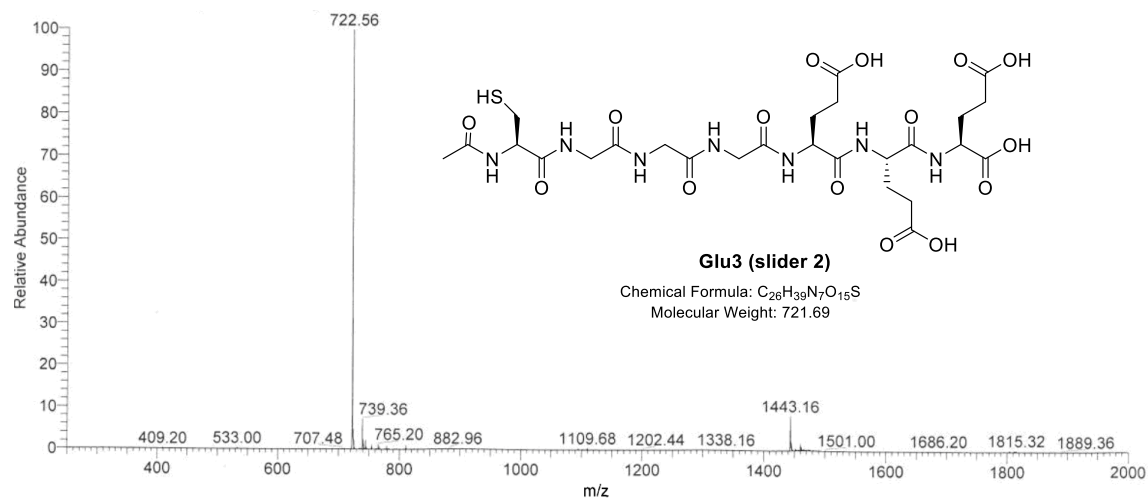
**Figure 14.** RP-HPLC trace for **Glu1**, detector (214 nm), gradient 1-100% (MeCN in 0.1% TFA of water), 0-30 min. Symbol \* stands for sample injection peak from system.



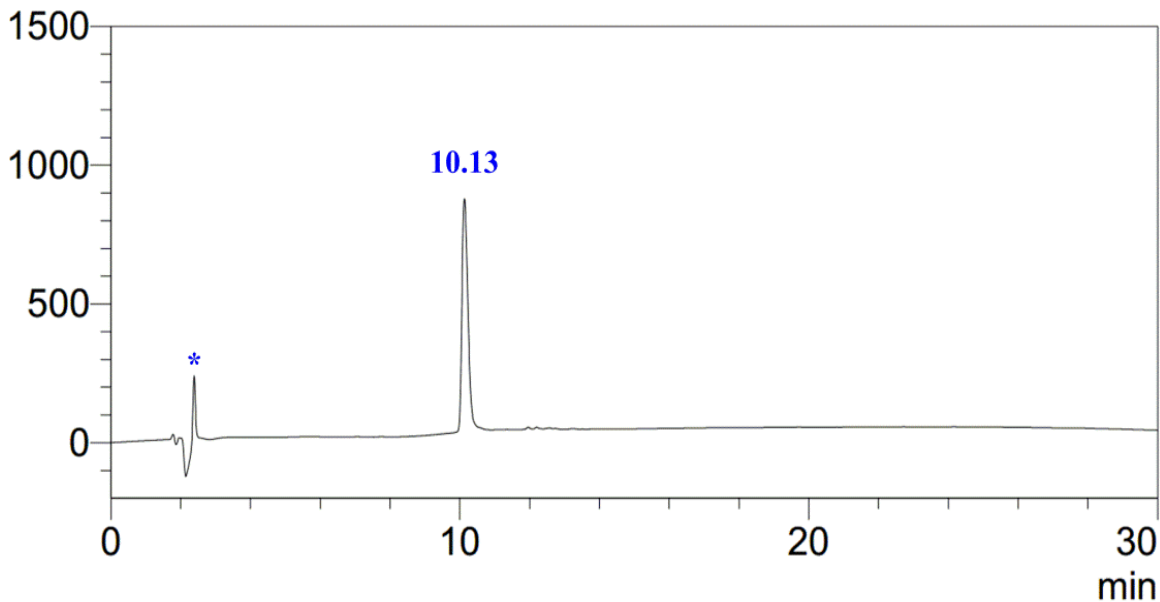
**Figure 15.** ESI-MS analysis of **Glu1**.



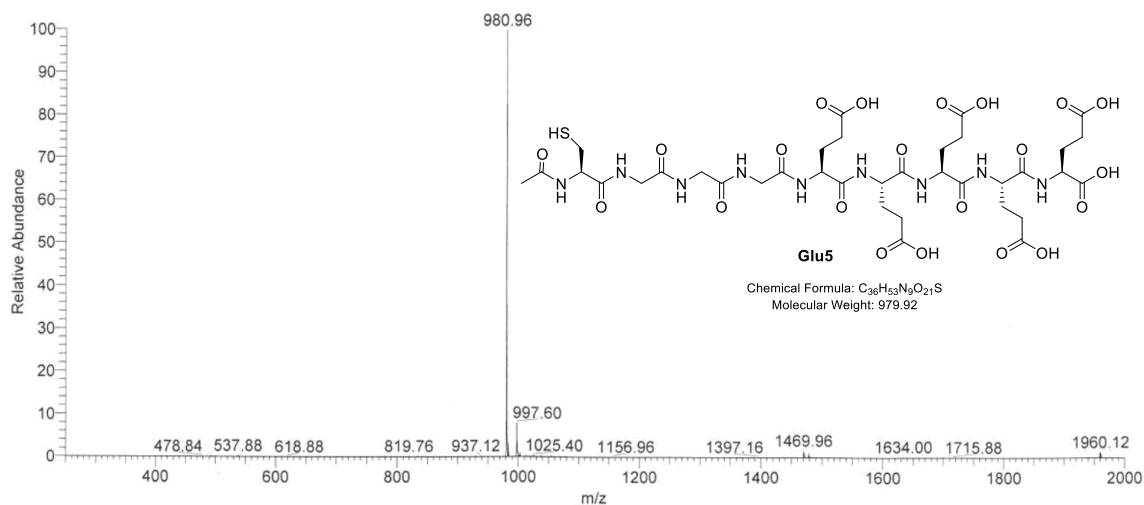
**Figure 16.** RP-HPLC trace for **Glu3 (slider 2)**, detector (214 nm), gradient 1-100% (MeCN in 0.1% TFA of water), 0-30 min. Symbol \* stands for sample injection peak from system.



**Figure 17.** ESI-MS analysis of **Glu3 (slider 2)**



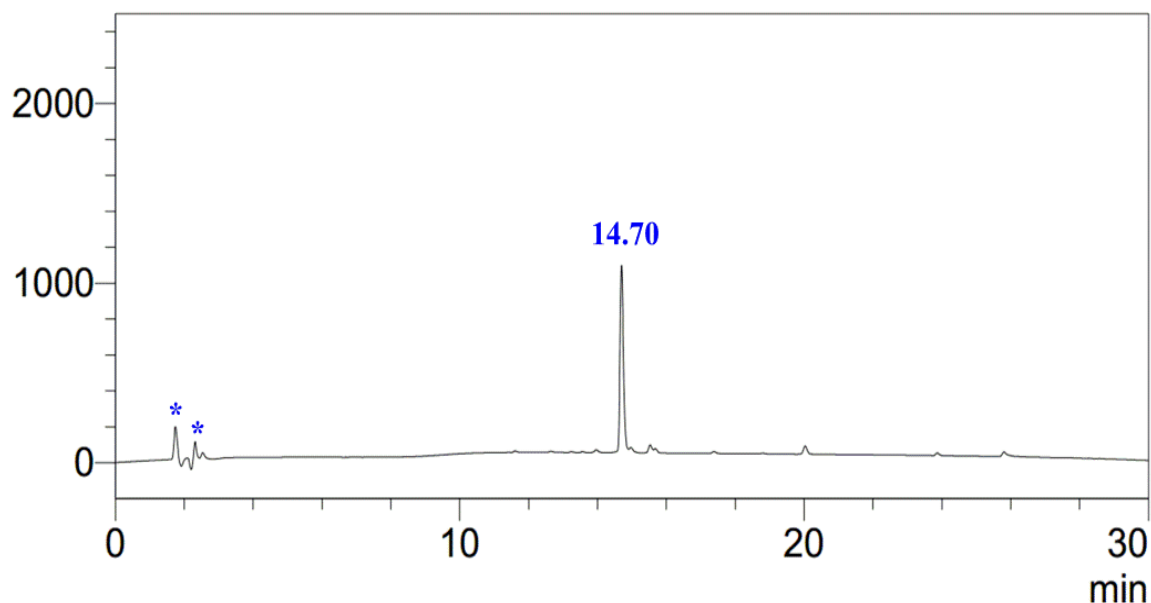
**Figure 18.** RP-HPLC trace for **Glu5**, detector (214 nm), gradient 1-100% (MeCN in 0.1% TFA of water), 0-30 min. Symbol \* stands for sample injection peak from system.



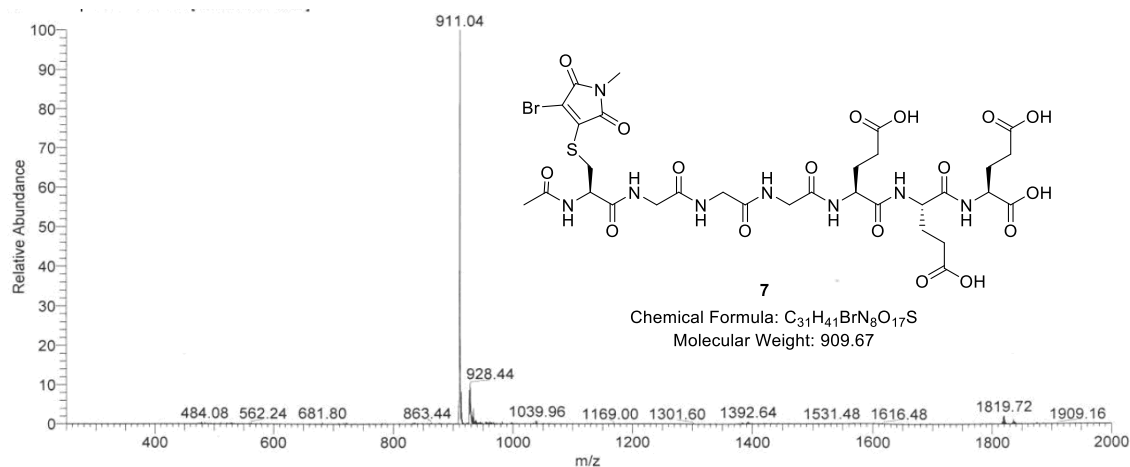
**Figure 19.** ESI-MS analysis of **Glu5**

### 3.6. Synthesis of bromo-substituted N-methyl-maleimide-**2** (**7**).

The synthesis of **7** was the same as the procedure for the synthesis of compound **5**. ESI MS  $m/z$ : mass calculated for  $C_{31}H_{41}BrN_8O_{17}S$   $[M+H]^+=910.67$ , found 911.04.



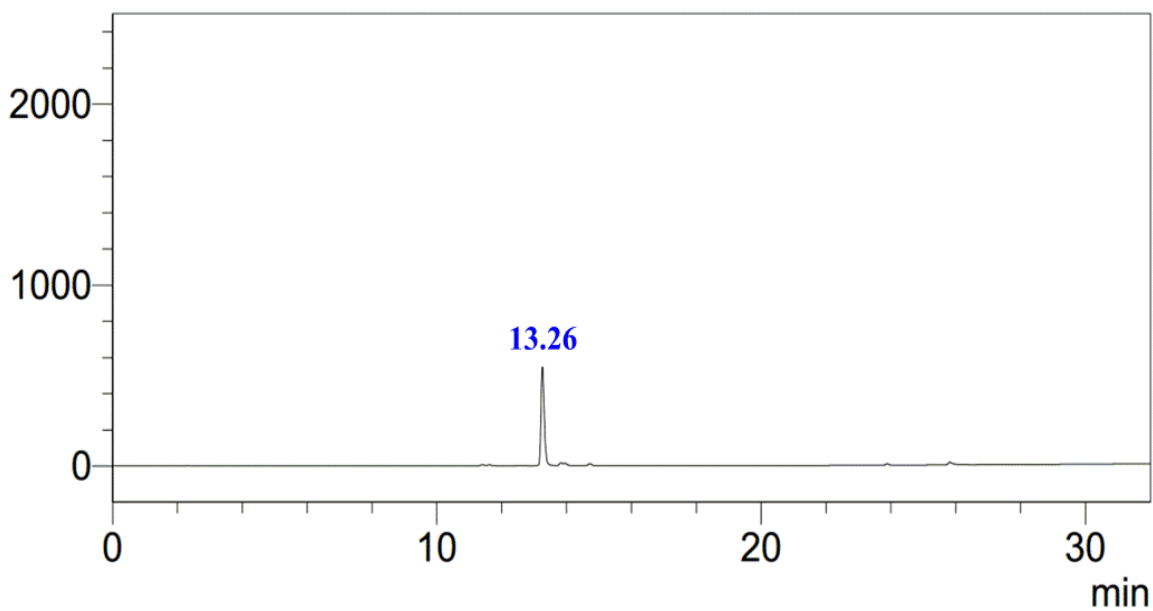
**Figure 20.** RP-HPLC trace for **7**, detector (214 nm), gradient 1-100% (MeCN in 0.1% TFA of water), 0-30 min. Symbol \* stands for sample injection peak from system.



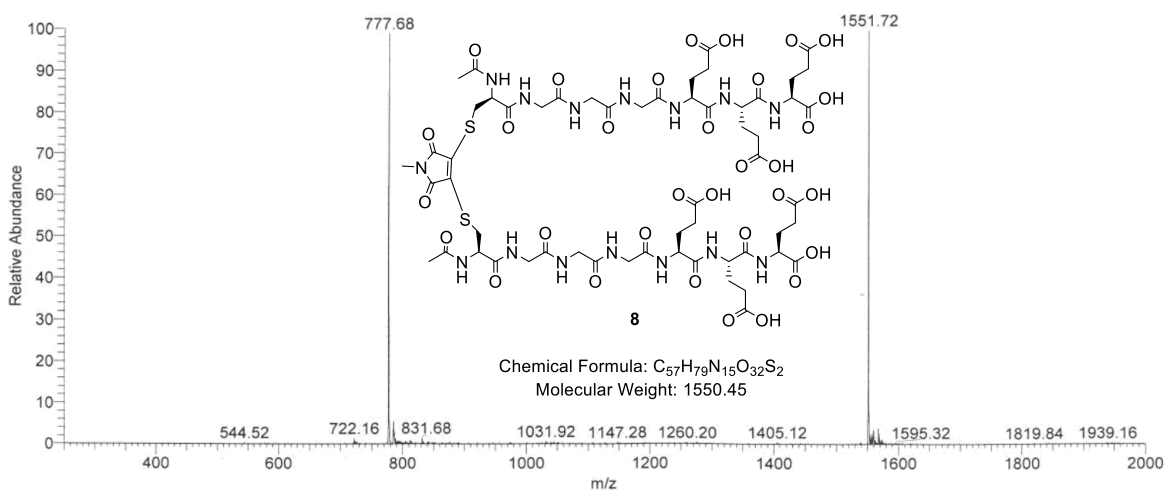
**Figure 21.** ESI-MS analysis of **7**.

### 3.7. Synthesis of slider **2** di-substituted N-methyl-maleimide (**8**).

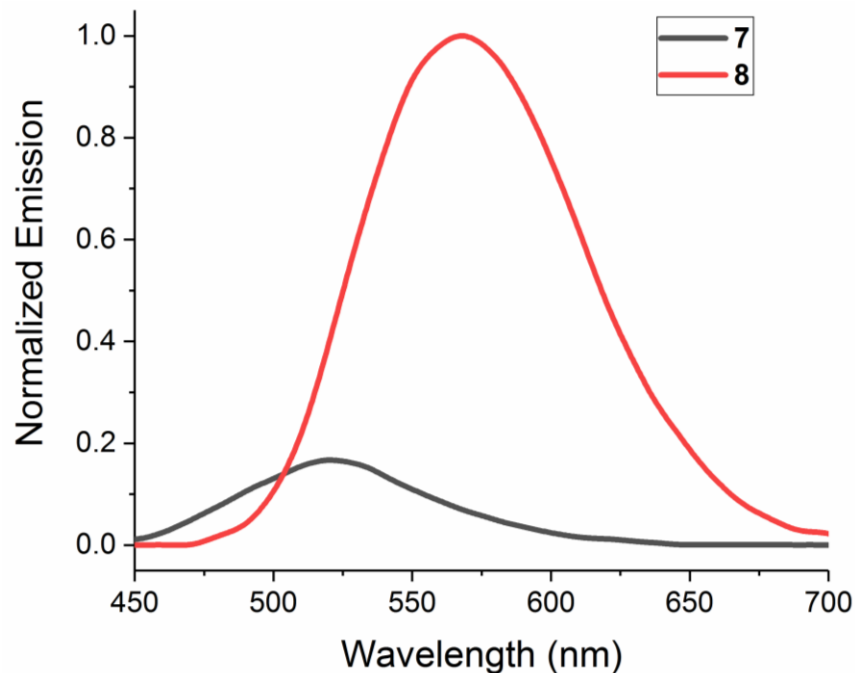
The synthesis of **8** was following the procedure for compound **6**. ESI MS m/z: mass calculated for  $C_{57}H_{79}N_{15}O_{32}S_2$   $[M+H]^+=1551.45$ , found 1551.72;  $[M+2H]^{2+}/2=776.23$ , found 777.68.



**Figure 22.** RP-HPLC trace for **8**, detector (254 nm), gradient 1-100% (MeCN in 0.1% TFA of water), 0-30 min.



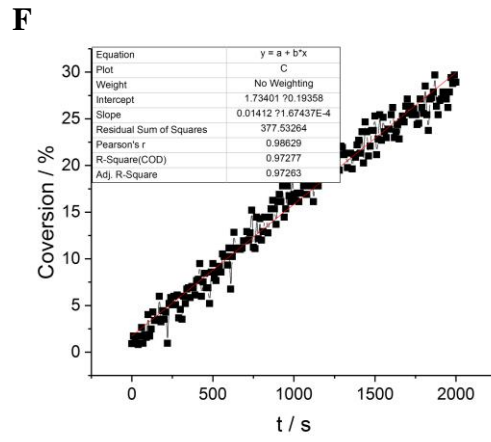
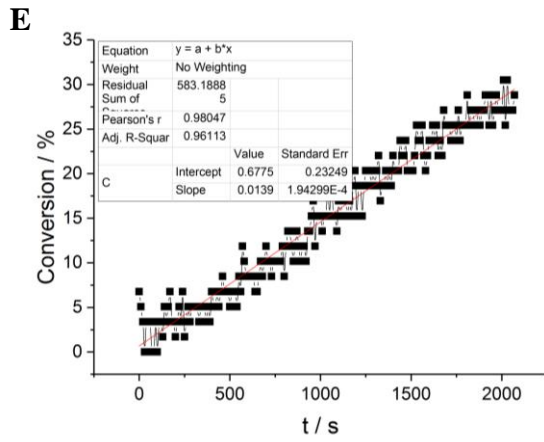
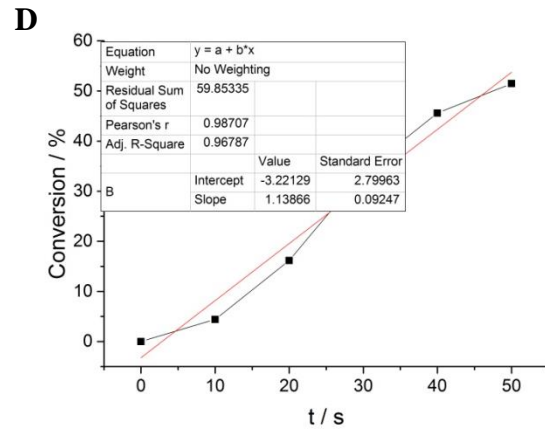
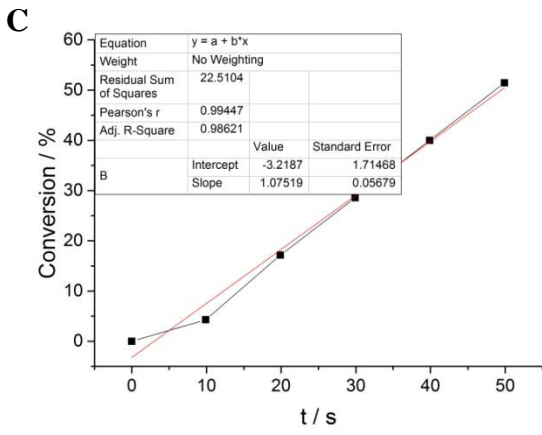
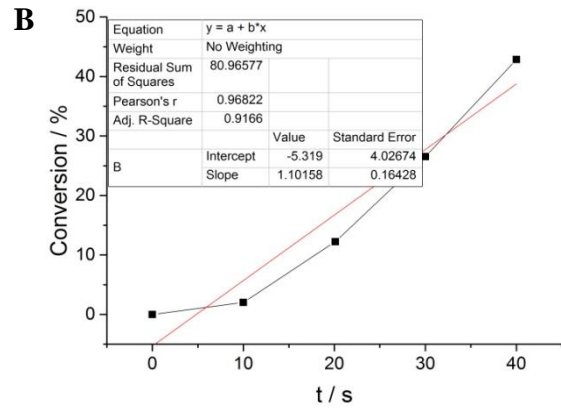
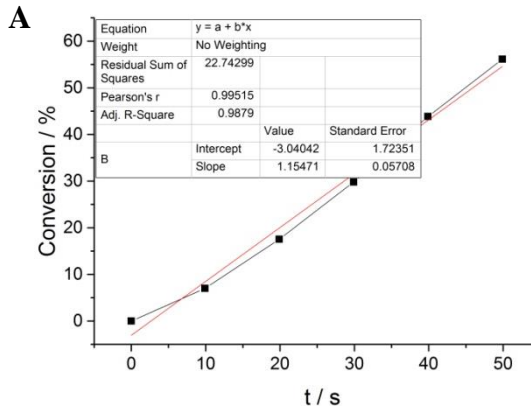
**Figure 23.** ESI-MS analysis of **8**.



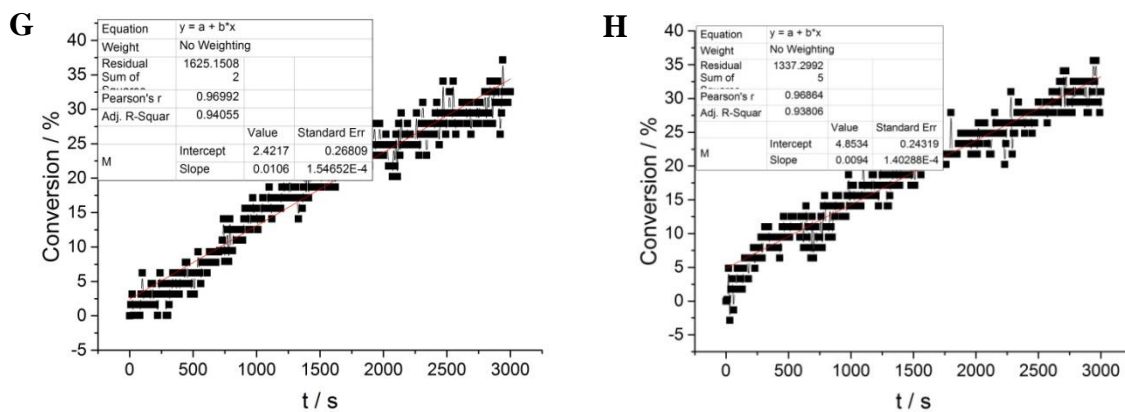
**Figure 24.** Emission spectra of **7** and **8** (0.1 mM in buffer), measurements were normalized to the higher intensity of **8**. Excitation wavelength: 416 nm.

### 3.8. Standard procedure for fluorogenic reaction in the presence or absence of polycations

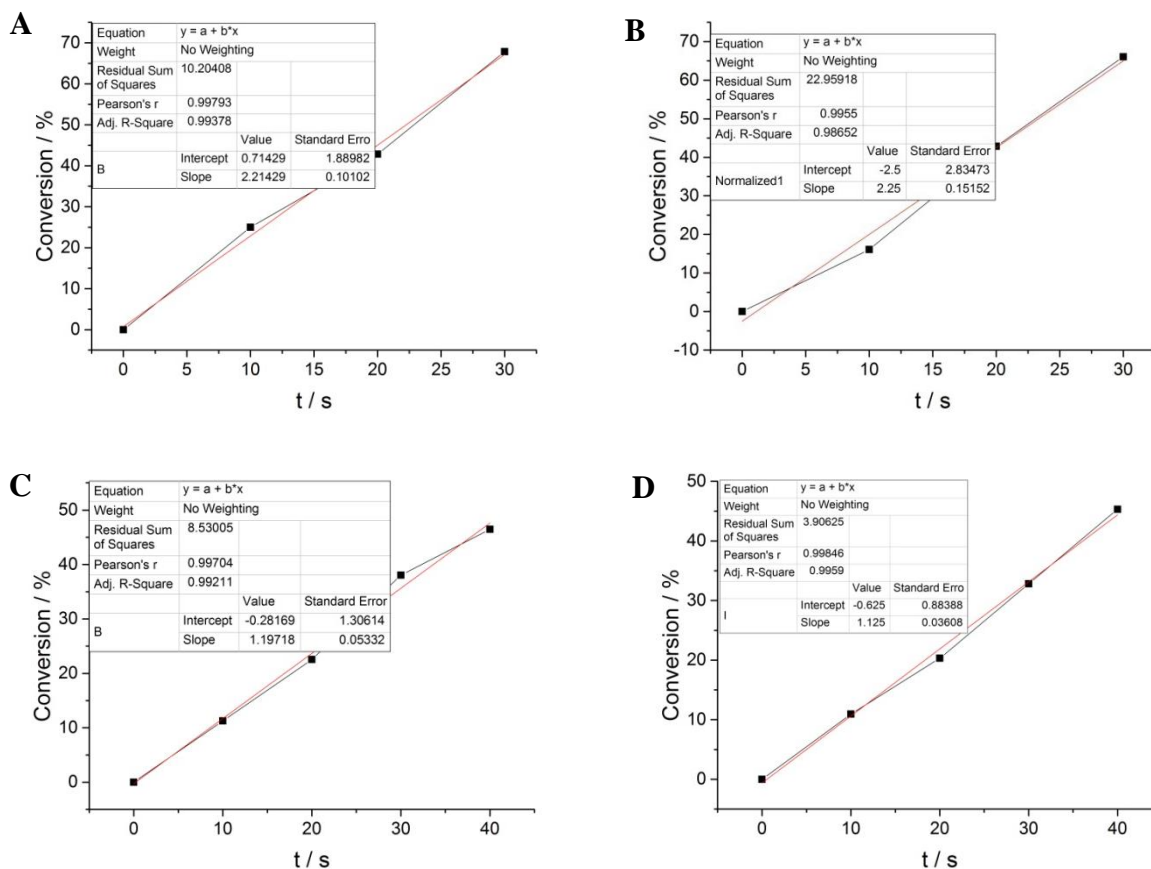
Bromo-substituted N-methyl-maleimide slider conjugates (2  $\mu\text{L}$  of 250  $\mu\text{M}$ ) and various amounts of polycations were pre-mixed in 50 mM MES or MOPS buffer in the absence or presence of sodium chloride. The final volume of these mixtures was 98  $\mu\text{L}$ . Then, 2.4  $\mu\text{L}$  of freshly prepared slider solutions (250  $\mu\text{M}$  stock) were added and the reaction kinetics was immediately recorded on a real time plate reader (excitation at 416 nm; emission at 600 nm).

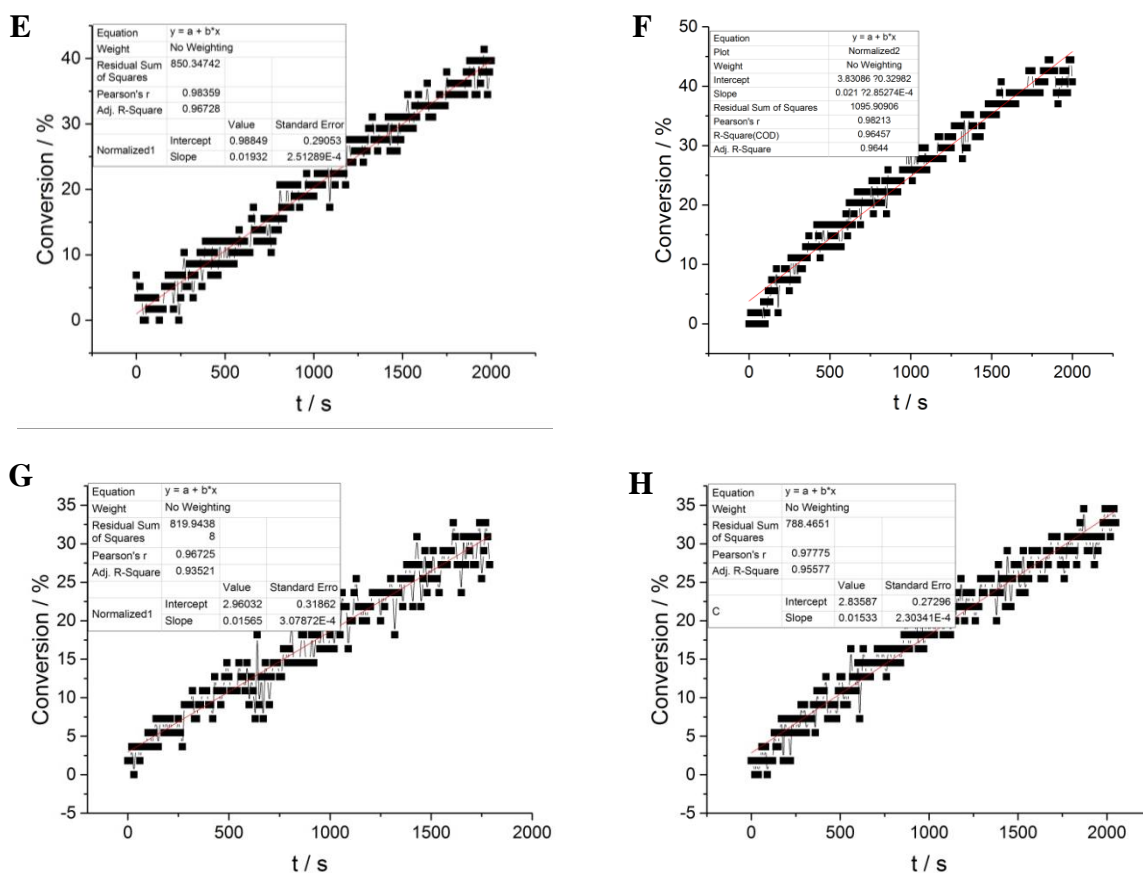




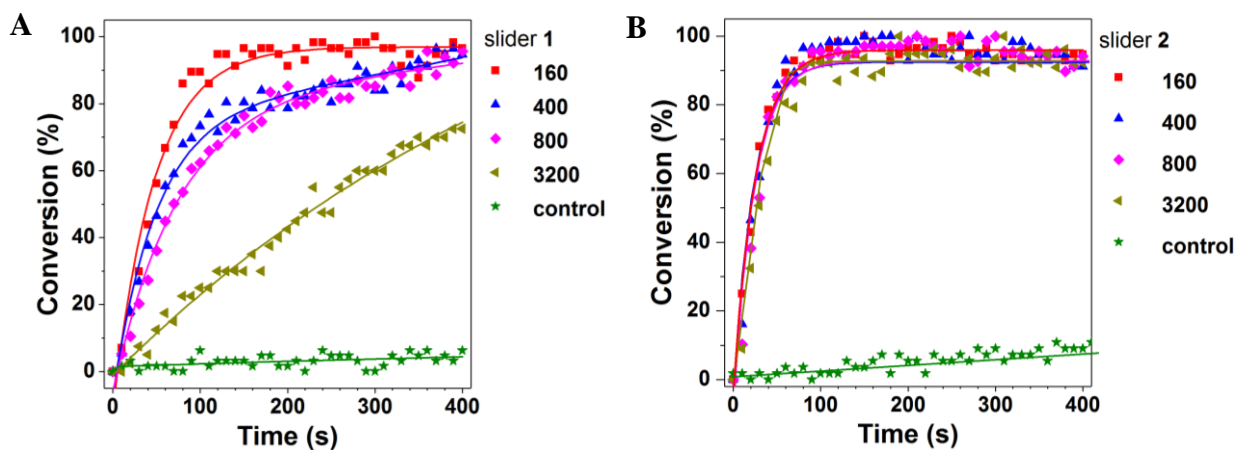


**Figure 25.** Determination of rate accelerations of the reactions between slider **1** and bromo-substituted N-methyl-maleimide-**1** in the presence of A), B) 1.76 mM pArg; C), D) 1.76 mM pLys; E), F) 1.76 mM Arginine and G), H) in the absence of polycations or cations. The relative rate accelerations were derived the slope of the emission of product vs. time for the first 30-50% of substrate conversion.

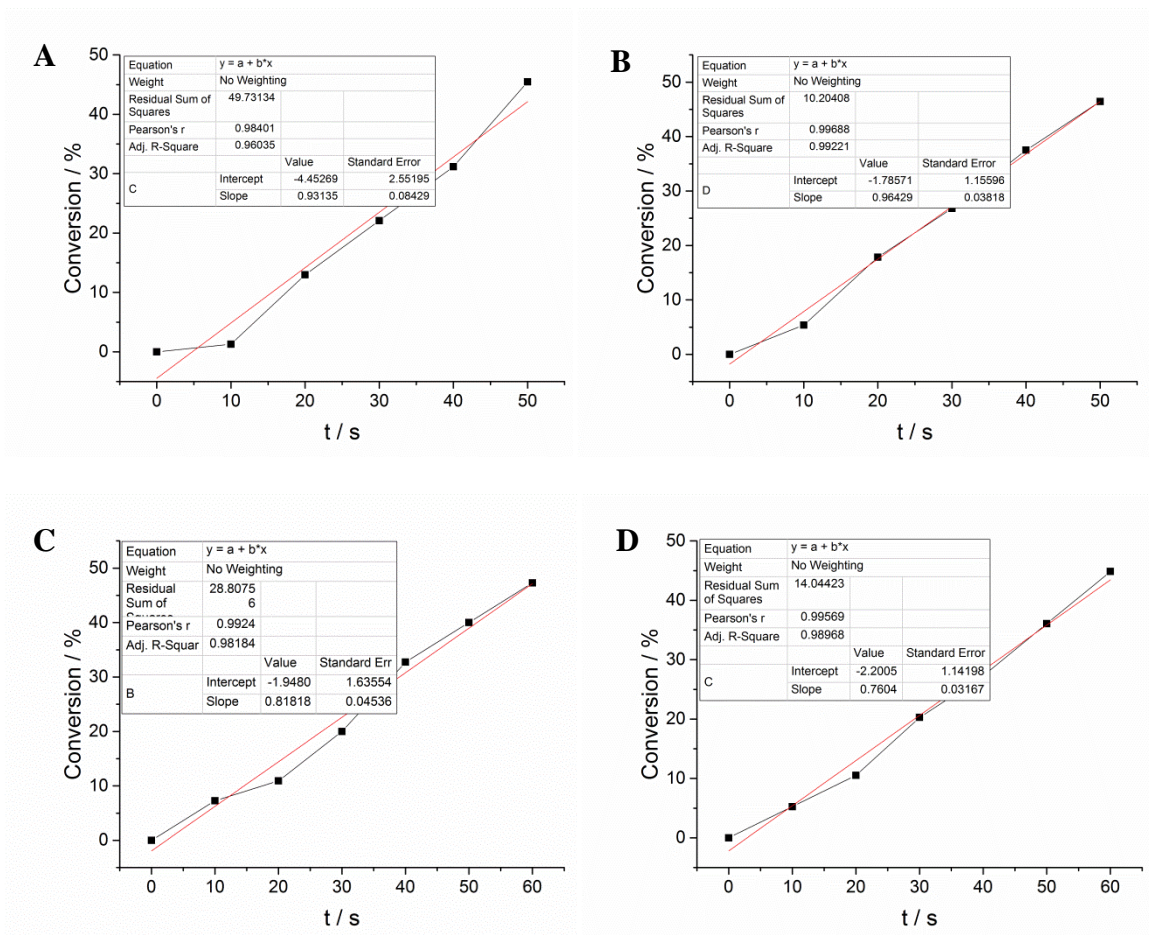


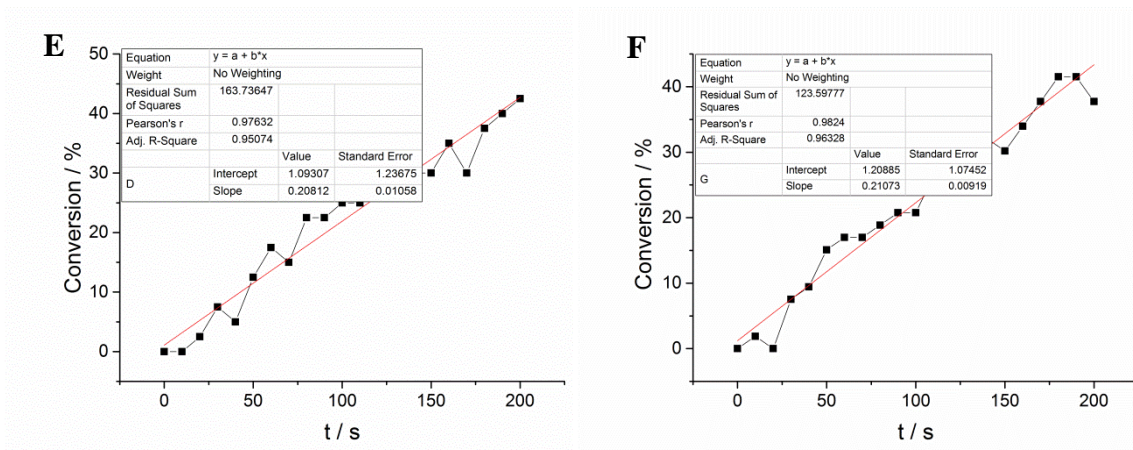


**Figure S26.** Determination of rate accelerations of the reactions between slider 2 and bromo-substituted N-methyl-maleimide-2 in the presence of A), B) 1.76 mM pArg; C), D) 1.76 mM pLys; E), F) 1.76 mM Arginine and G), H) in the absence of polycations or cations. The relative rate accelerations were derived the slope of the emission of product *vs.* time for the first 30-50% of substrate conversion.

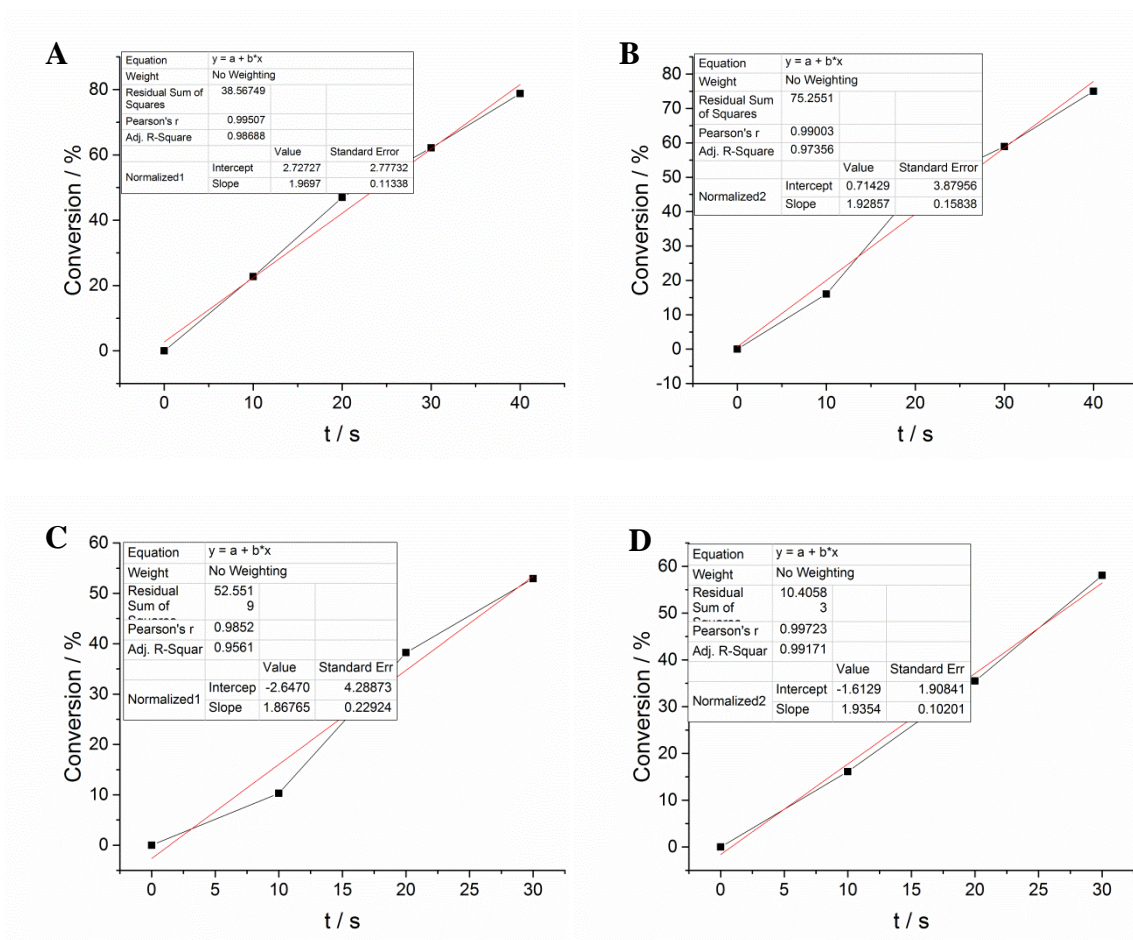


**Figure 27.** Kinetics of reaction between: **A)** slider 1 and bromo-substituted N-methyl-maleimide-1 in the presence of pArg,  $N_{\text{Arg}}$  vs  $N_{\text{slider}}$  ratios of 160, 400, 800 and 3200; **B)** slider 2 and bromo-substituted N-methyl-maleimide-2 in the presence of pArg,  $N_{\text{Arg}}$  vs  $N_{\text{slider}}$  ratios of 160, 400, 800 and 3200.





**Figure 28.** Determination of rate accelerations of the reactions between slider **1** and bromo-substituted N-methyl-maleimide-**1** in the presence of A), B) 4.4 mM pArg ( $N_{\text{Arg}} : N_{\text{slider 1}} = 400$ ); C), D) 8.8 mM pArg ( $N_{\text{Arg}} : N_{\text{slider 1}} = 800$ ) and E), F) 35.2 mM pArg ( $N_{\text{Arg}} : N_{\text{slider 1}} = 3200$ ). The relative rate accelerations were derived the slope of the emission of product vs. time for the first 30-50% of substrate conversion.





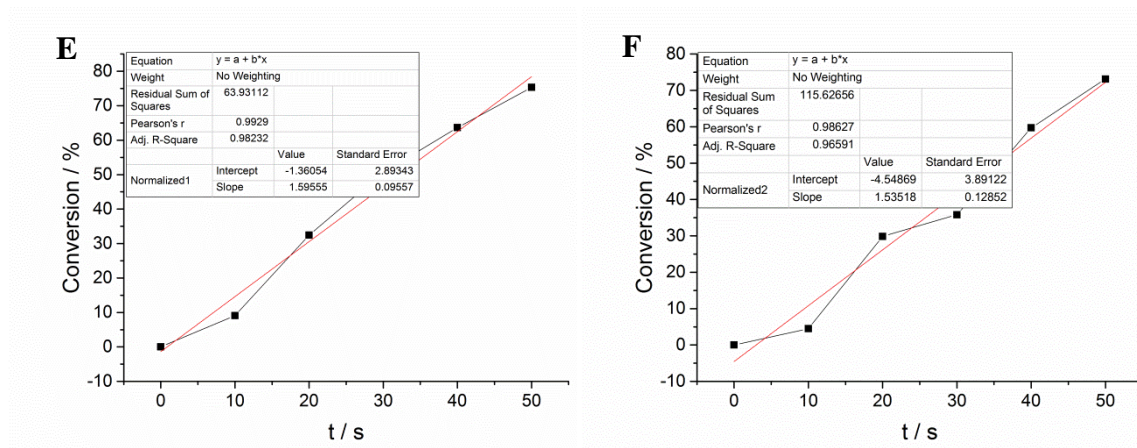


**Figure 29.** Determination of rate accelerations of the reactions between slider 2 and bromo-substituted N-methyl-maleimide-2 in the presence of A), B) 4.4 mM pArg ( $N_{\text{Arg}} : N_{\text{slider 2}} = 400$ ); C), D) 8.8 mM pArg ( $N_{\text{Arg}} : N_{\text{slider 2}} = 800$ ) and E), F) 35.2 mM pArg ( $N_{\text{Arg}} : N_{\text{slider 2}} = 3200$ ). The relative rate accelerations were derived the slope of the emission of product vs. time for the first 60-80% of substrate conversion.

**Table 2.** Relative rate accelerations in the presence of polycations.

Catalyst	slider 1		slider 2	
	slope	Rate acceleration	slope	Rate acceleration
none	0.010±0.001	1	0.015±0.001	1
Arg(160)	0.014	1.4	0.020±0.001	1.3
pArg(160)	1.13±0.03	113	2.23±0.02	149
pArg(400)	0.94±0.02	94	1.95±0.02	130
pArg(800)	0.79±0.03	79	1.90±0.03	127
pArg(3200)	0.21	21	1.56±0.04	104
pLys(160)	1.10±0.03	110	1.16±0.04	77

All error bars are the result of two independent measurements.

### 3.9. Dependence of fluorogenic reaction rates on NaCl concentrations

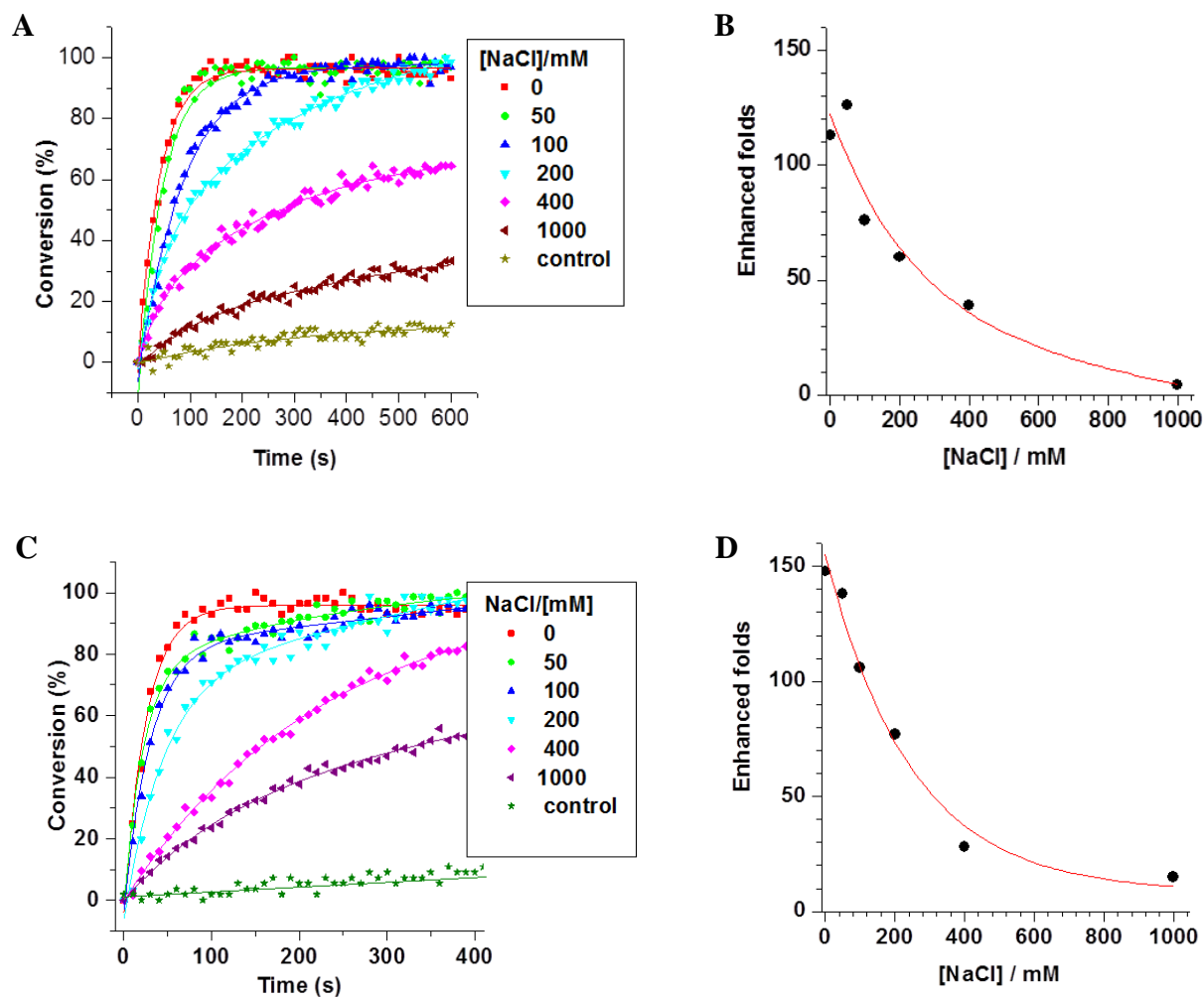


**Figure 30.** A) Reaction kinetics of slider 1 reacting with bromo-substituted N-methyl-maleimide-1 in the presence of 1.76 mM pArg in the presence of 0, 50, 100, 200, 400 and 1000 mM NaCl; B) The dependence of rate acceleration of slider 1 reacting with bromo-substituted N-methyl-maleimide-1 on the concentration of NaCl. C) Reaction kinetics of slider 2 reacting with bromo-substituted N-methyl-maleimide-2 in the presence of 1.76 mM pArg in the presence of 0, 50, 100, 200, 400 and 1000 mM NaCl; D) The dependence of rate acceleration of slider 2 reacting with bromo-substituted N-methyl-maleimide-2 on the concentration of NaCl.

## 4. Molecular Dynamic Simulations

### 4.1. Systems and methods

Atomistic molecular dynamics (MD) simulations of molecular sliders diffusion on polycation tracks were performed to clarify the observed enhancement of reaction rates between sliders and their bromo-substituted N-methyl-maleimide conjugates, which takes part on polycation tracks. The following cases were simulated: slider **1**-pArg/pLys, with one slider **1** and one polyArginine/polyLysine track of 95 Arginine/Lysine residues placed in a 25 mM MES solution; slider **2**-pArg/pLys, with one slider **2** and one polyArginine/polyLysine track of 95 Arginine/Lysine residues placed in a 22 mM MOPS solution. A 95-residues long track with a molecular weight of ~15,000 Da was selected to represent a polycation track. The positive charge arising from the polycation chain is close to 96 mM (3,000 folds larger than the dissociation constant of slider), which means that a slider practically does not leave the polycations during the simulations.

The diffusion of sliders on polycation tracks was simulated by NAMD2<sup>2</sup> and the CHARMM general force field<sup>3,4</sup>. After performing a geometry optimization at MP2 level by GAUSSIAN 09<sup>5</sup>, the charges and dihedrals parameters in the tail of slider **1** (between the thiol group and phosphate group) were separately calculated by a Force Field Toolkit<sup>6</sup> from VMD<sup>7</sup>. The polycation tracks were described by a CHARMM36<sup>8,9</sup> force field. The Particle Mesh Ewald (PME)<sup>10</sup> method was used for the evaluation of long-range Coulombic interactions. The time step was set to 2.0 fs. The simulations were performed in the NPT ensemble ( $p = 1$  bar and  $T = 300$  K), using the Langevin dynamics ( $\gamma_{\text{Lang}} = 1$  ps<sup>-1</sup>). After 2,000 steps of minimization, ions and water molecules were equilibrated for 2 ns around sliders and tracks, which were restrained using harmonic forces with a spring constant of 1 kcal/(mol Å<sup>2</sup>). The last frames of restrained equilibration were used to start simulations of free sliders and tracks. Then, 200 ns trajectories were used to compute MSD at a variety of lag times ( $\tau$ ). A diffusion coefficient  $D(\tau)$  was computed from  $D(\tau) = \text{MSD}(\tau) / 2E\tau$ , where  $E$  is the integer dimensionality of the system (1, 2 or 3)<sup>11</sup>. The H-bonds number was analyzed by VMD<sup>7</sup> with a cutoff distance of 3.5 Å and angle of 60°.

The free energy calculation was performed using an umbrella sampling (US) method. The coordinate, which was defined as the distance between the center of charged groups of slider and the center of pArg track (11 units of ARG), was partitioned into 40 windows of 1 Å width, where confinement potentials were introduced in the forms of harmonic restraints with force constants of 3 kcal/(mol Å<sup>2</sup>). During sampling, three backbone atoms of pArg track were held by restraints, implemented by means of collective variable module (colvars<sup>12</sup>). Each US window was run for 10 ns. The weighted histogram analysis method (WHAM<sup>13, 14</sup>) was used to reconstruct the potential of mean force (PMF). A Monte Carlo bootstrap error analysis was performed with the WHAM algorithm (with num\_MC\_trials set to 3). The histograms of the US windows used to reconstruct the PMF were examined and shown to have an appropriate overlap.



## 4.2. Trajectories of sliders on polycation tracks

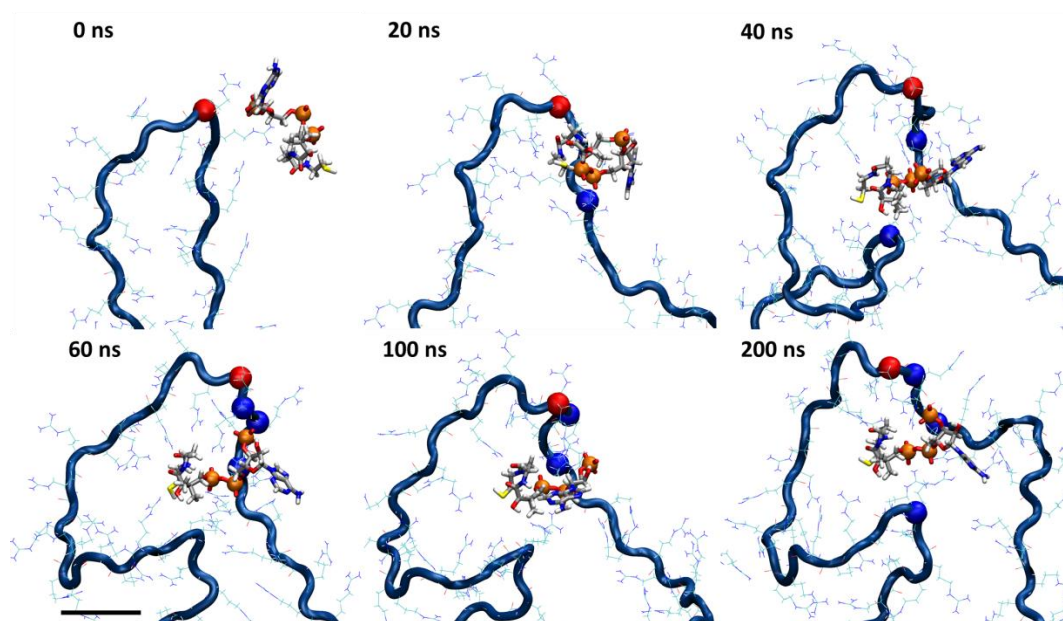


**Figure 31.** Slider 1 on pArg track. Track is shown in dark blue with side chains of Arg, and slider is shown in grey, with P atom in orange, O in red, N in blue, S in yellow and H in white. Red point on the track is the initial nearest backbone atom from track to slider, and blue points are the backbone atoms within 7 Å of slider during the simulation. Scale bar 1 nm.

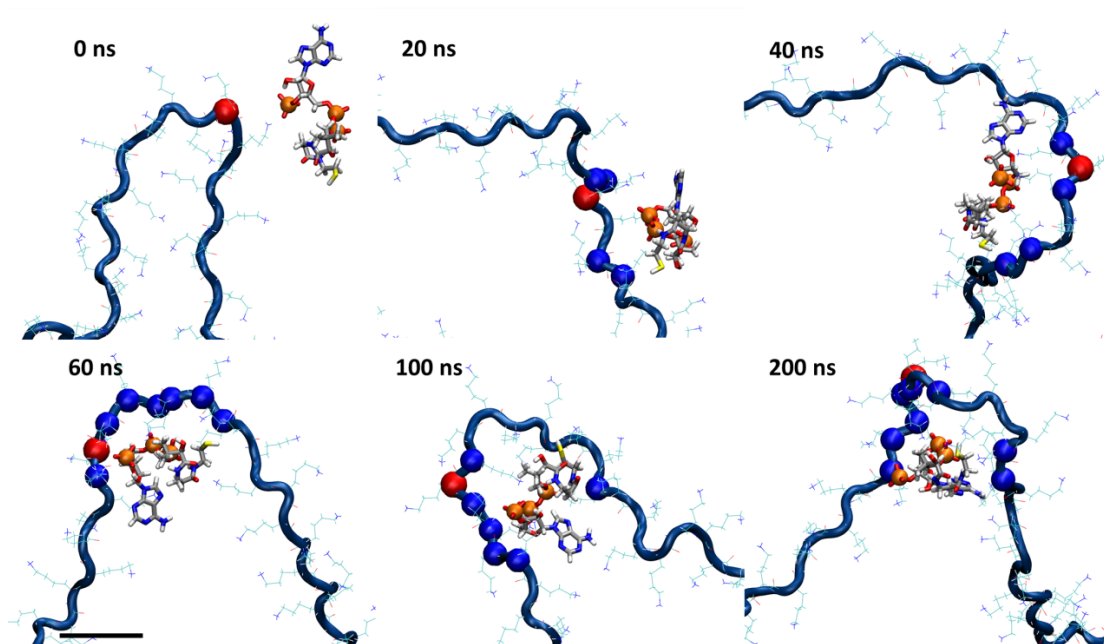


**Figure 32.** Slider 1 on pLys track. Track is shown in dark blue with side chains of Lys, and slider is shown in grey, with P atom in orange, O in red, N in blue, S in yellow and H in white. Red point

on the track is the initial nearest backbone atom from track to slider, and blue points are the backbone atoms within 7 Å of slider during the simulation. Scale bar 1 nm.

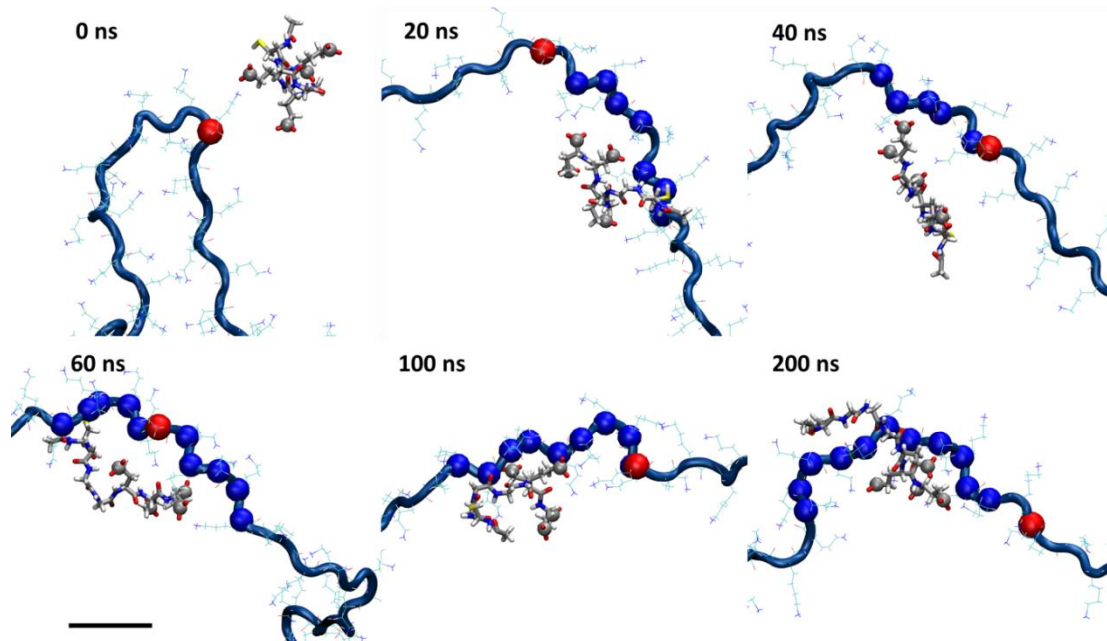


**Figure 33.** Slider 2 on pLys track. Track is shown in dark blue with side Lys chain, and slider is shown in grey, with C atom of carboxyl group in sphere, O in red, N in blue, S in yellow and H in white. Red point on the track is the initial nearest backbone atom from track to slider, and blue points are the backbone atoms within 7 Å of slider during the simulation. Scale bar 1 nm.

#### 4.3 Motion of polycation tracks caused by sliders

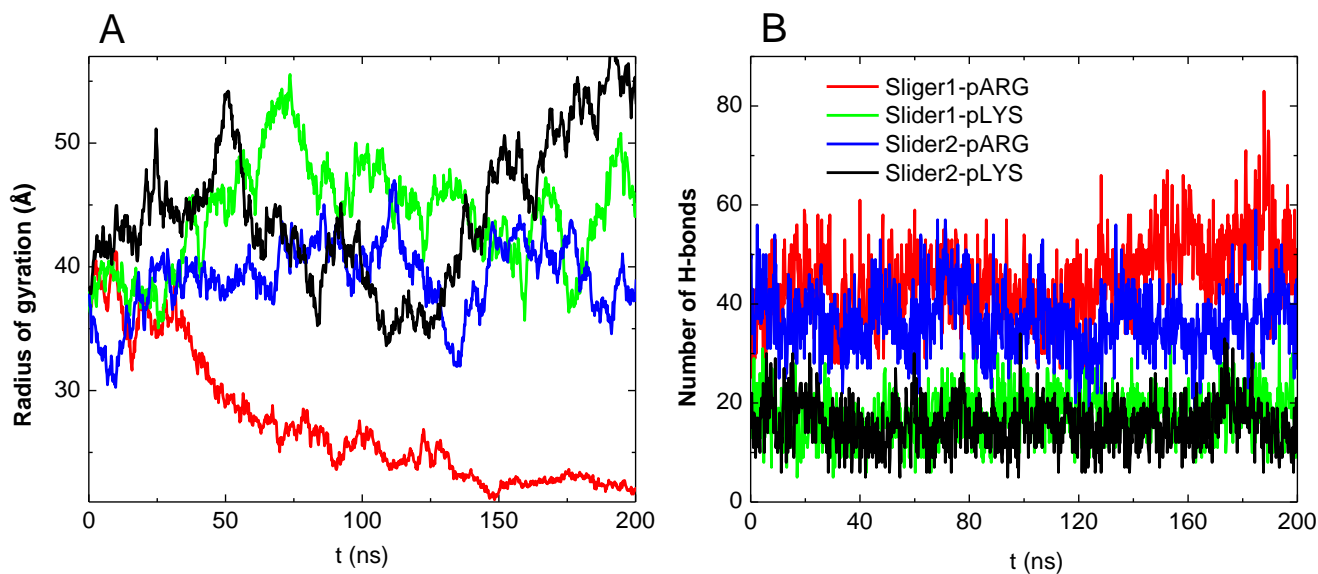


**Figure 34** A) Radius of gyration; B) number of H-bonds within polycation track.

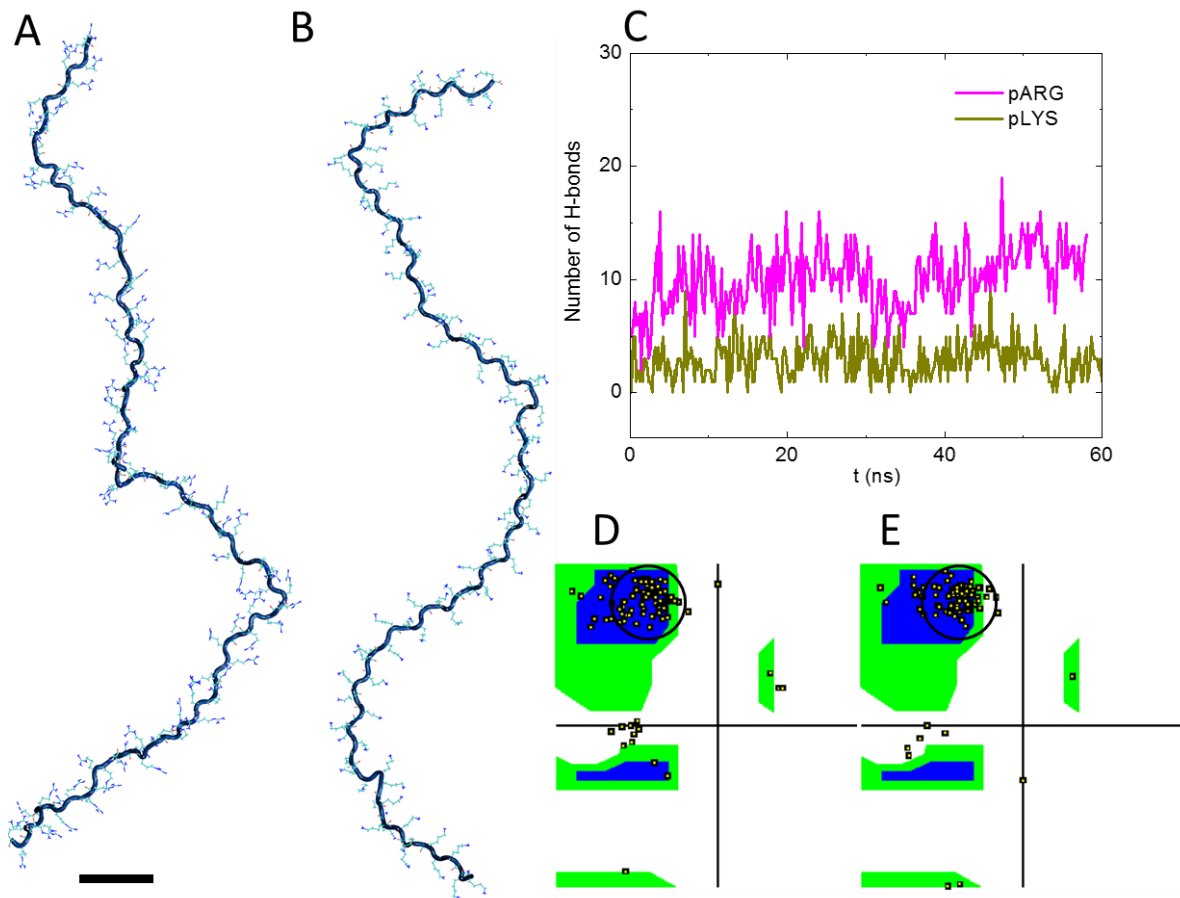


**Figure 35.** Structure information of pArg and pLys tracks without slider (simulation time of 60 ns). A) pArg track; B) pLys track; C) number of H-bonds within polycation track itself; D) pArg Ramachandran plot at 60 ns; E) pLys Ramachandran plot at 60 ns. Scale bar is 2 nm and the PPII helix region is circled.

#### 4.4 Inter-track hopping of sliders

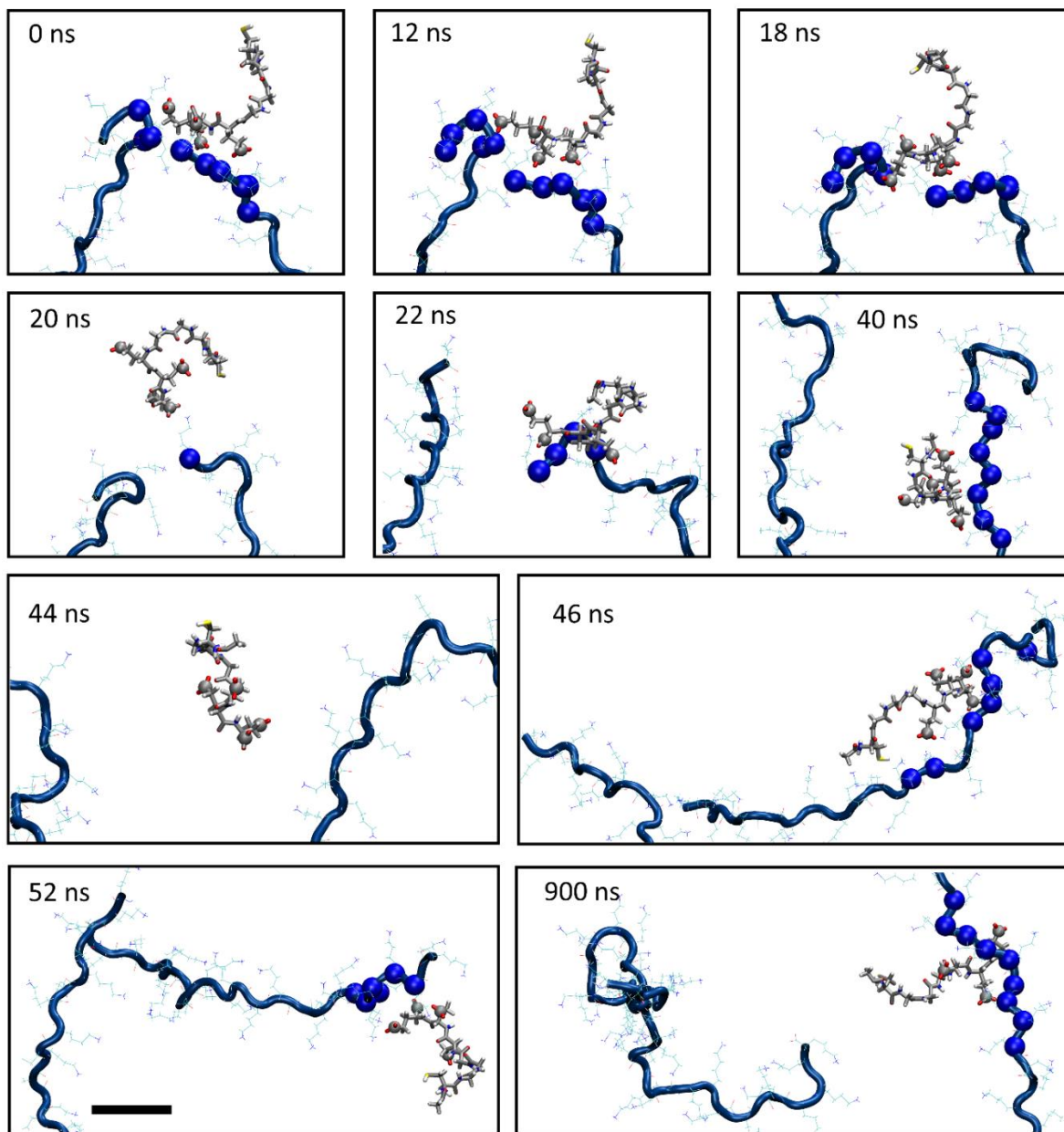


**Figure 36.** Snapshots of slider **2** interacting with two short pLys tracks. Track is shown in dark blue with side chains, and slider is shown in grey, with C atom of carboxyl group in sphere, O in red, N in blue, S in yellow and H in white. Blue points are the backbone atoms within 7 Å of slider during the simulation. Scale bar 1 nm.

#### 4.5 Free energy calculation

We assume that the average contact number per second is equal to the Arrhenius frequency, which is predicted from the average contact number between sliders and side chains of polycation track

(Table S3). The contact number, defined as the number of side chains of polycation track within 4 Å of slider charged group, was collected every 0.2 ns in Figure S38.

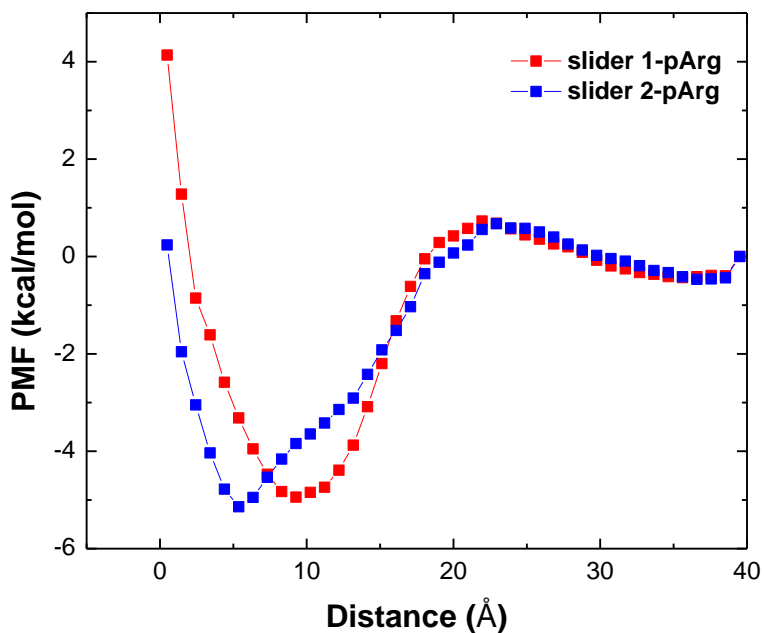


**Figure 37.** Free energy profile of slider1/2 unbinding from the pArg track. The distance between centers of mass of charged groups of slider and pARG track is defined as reaction coordinate.

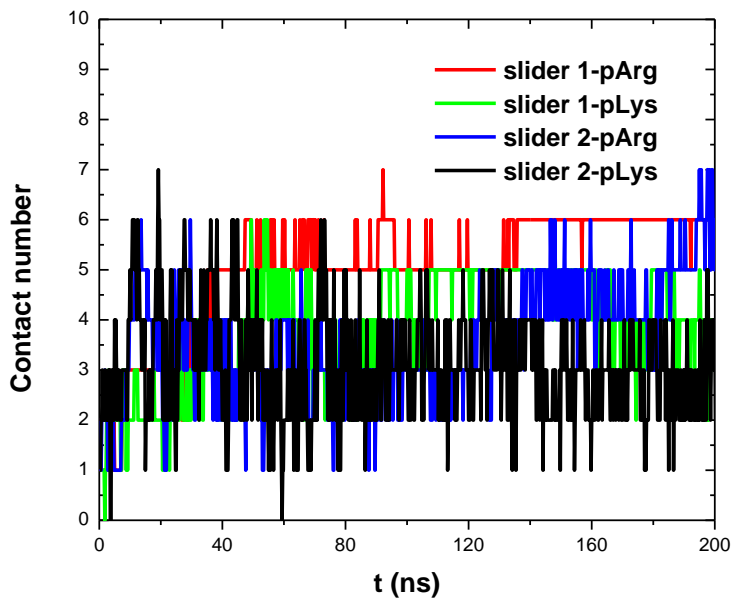


**Figure 38.** The contact number between slider charged groups and side chains of pArg/Lys during 200 ns trajectory (data collect every 0.2 ns).

**Table 3.** Average contact number and Arrhenius frequency

	pArg • slider 1	pArg • slider 2	pLys • slider 1	pLys • slider 2
Average contact number	5.0	3.9	3.8	3.1
Arrhenius frequency (s <sup>-1</sup> )	2.5×10 <sup>10</sup>	2.0×10 <sup>10</sup>	1.9×10 <sup>10</sup>	1.6×10 <sup>10</sup>

## 5. Inter-track molecular cargo transport

### 5.1. Syntheses of donor tracks

Taking Arg<sub>18</sub>-S-Acetyl as an example, the synthesis procedure is as following: 6 mg Arg<sub>18</sub>-SH (2 μmol) and 5 mg TCEP (20 μmol) were dissolved in 800 μL of MOPS buffer (50 mM pH 7.1). Then, 16 mg acetic acid N-hydroxysuccinimide (NHS) ester (100 μmol) in 200 μL of DMF were added. The reaction mixture was shaken for 12 h at room temperature under Argon. After that, the crude product was purified by dialysis (MWCO 3500D) and further characterized by MALDI-TOF MS.

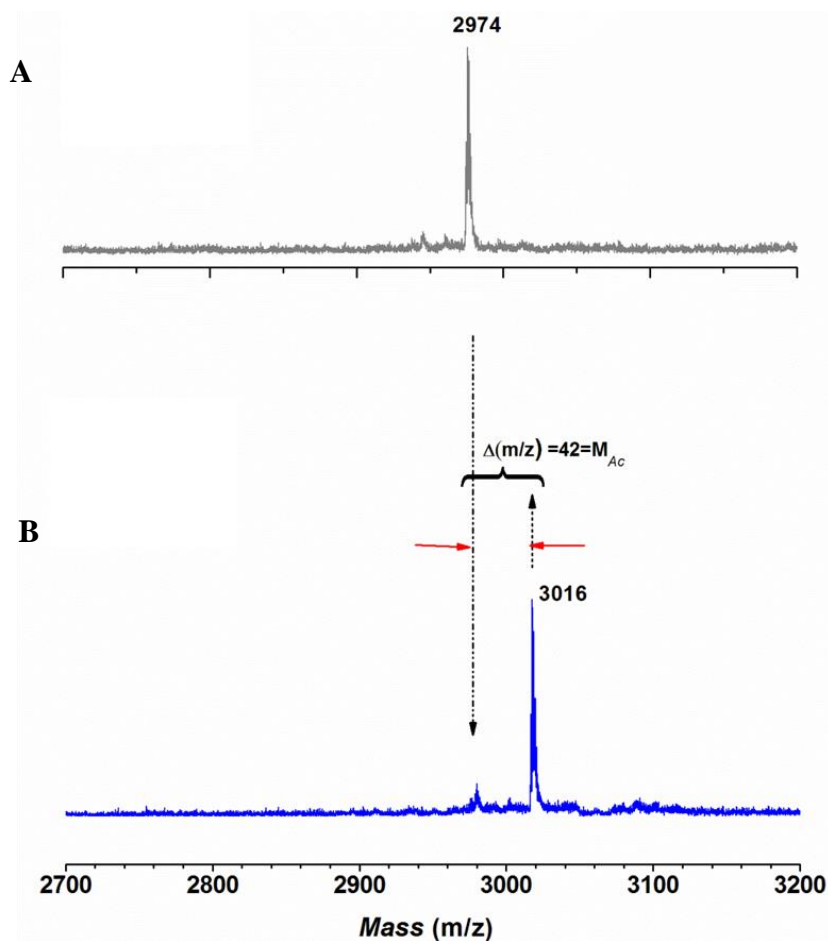
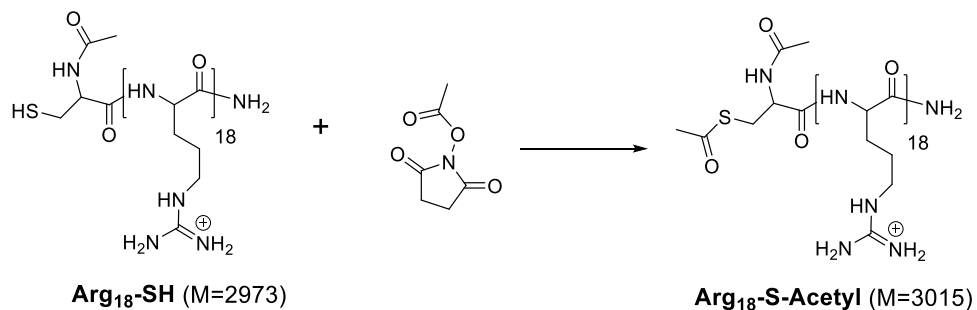


**Figure 39.** MALDI-TOF mass spectra of A) the starting material Arg<sub>18</sub>-SH that was synthesized by solid phase peptide synthesis; and B) Arg<sub>18</sub>-S-Acetyl.

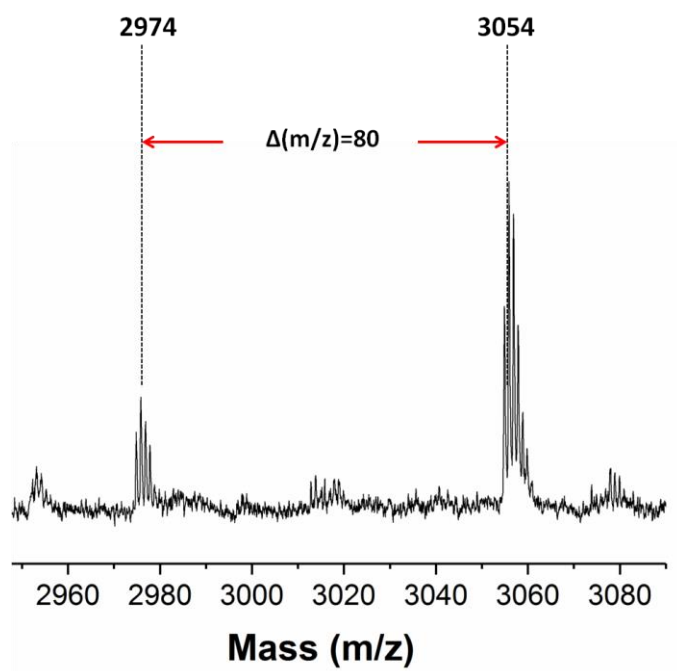
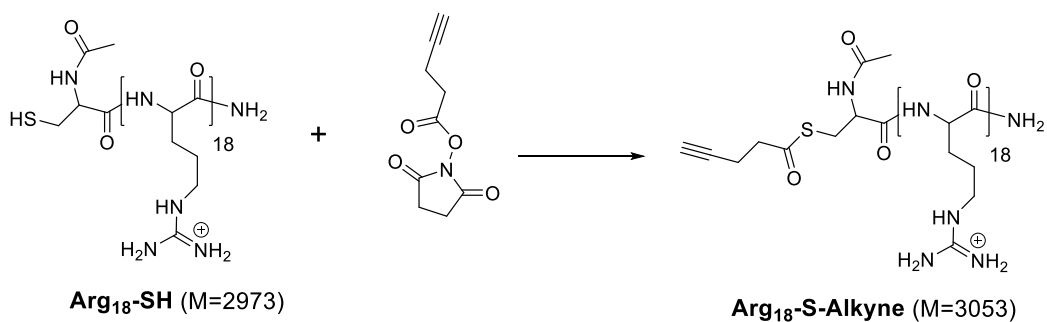


**Figure 40.** MALDI-TOF mass spectra of Arg<sub>18</sub>-S-Alkyne.



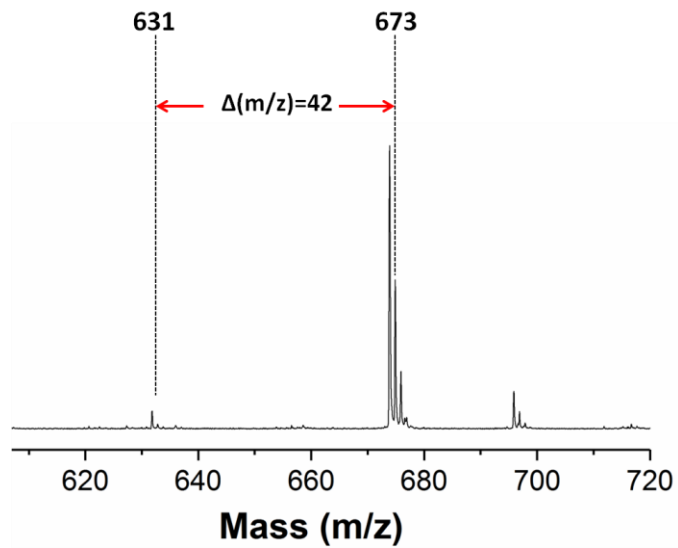
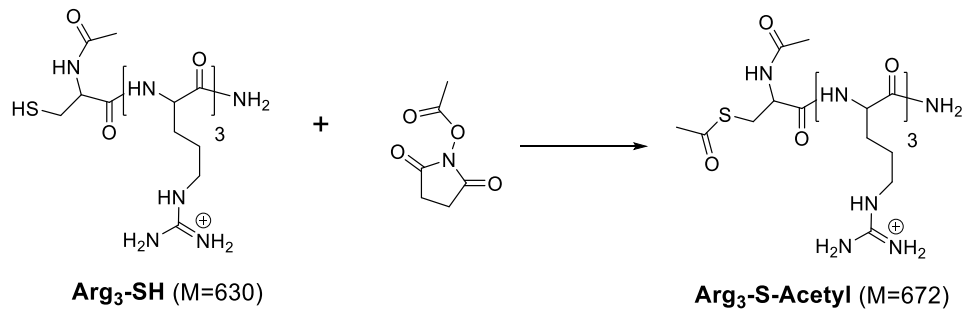


**Figure 41.** MALDI-TOF mass spectra of Arg<sub>3</sub>-S-Acetyl.

## 5.2. Proof of picking up acetyl group

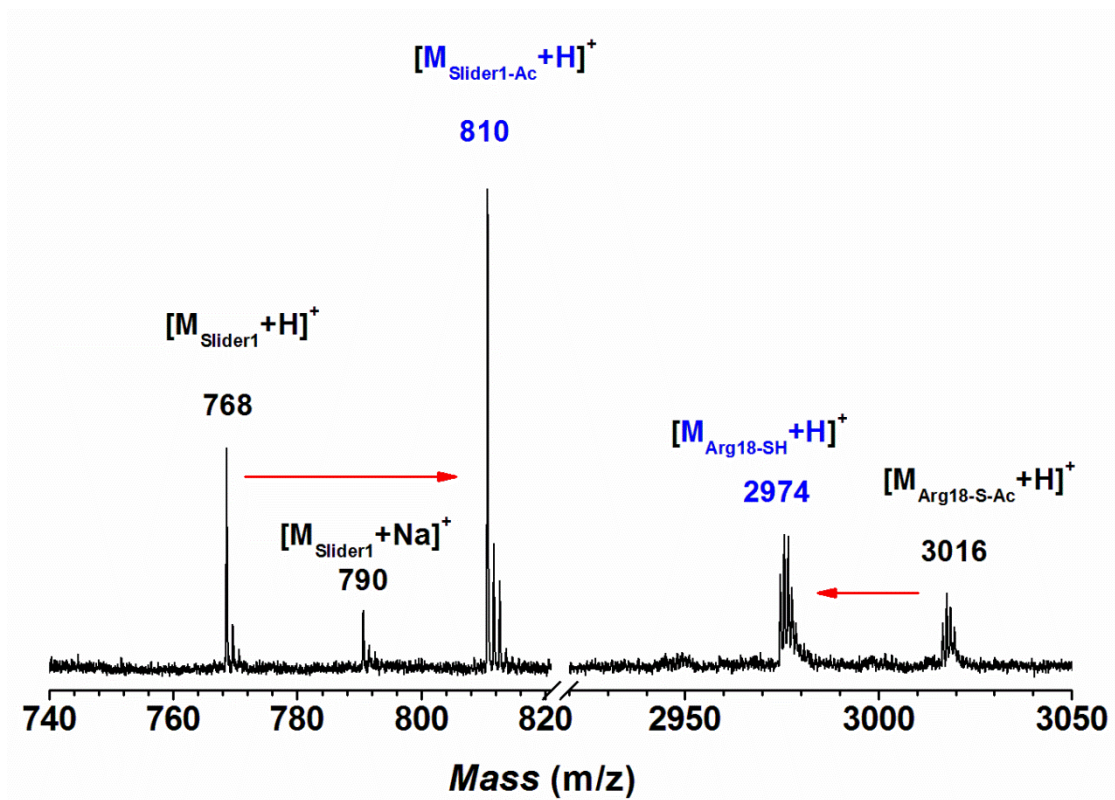
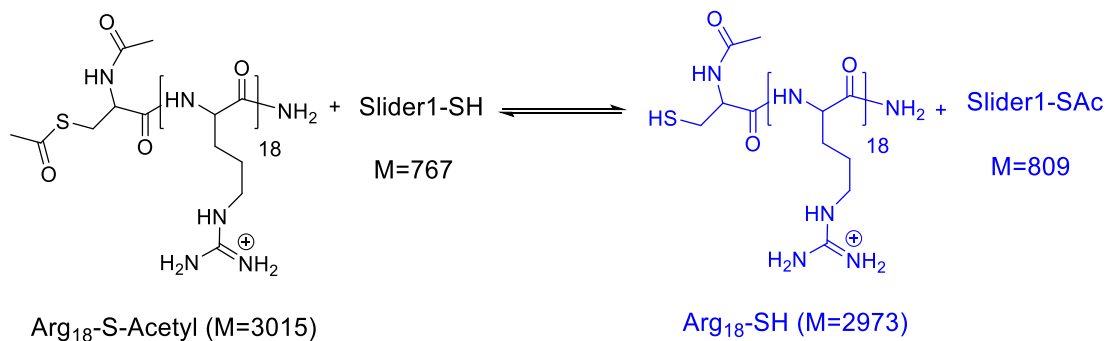


**Figure 42.** MALDI-TOF mass spectra of the reaction mixture of slider **1** (10  $\mu\text{M}$ ) and Arg<sub>18</sub>-S-Acetyl (10  $\mu\text{M}$ ) in MOPS buffer (10 mM, pH 7.1) after 1h. New peaks corresponding to slider **1**-SAc and Arg<sub>18</sub>-SH were marked in blue.

### 5.3. Proof of acetyl group deposition

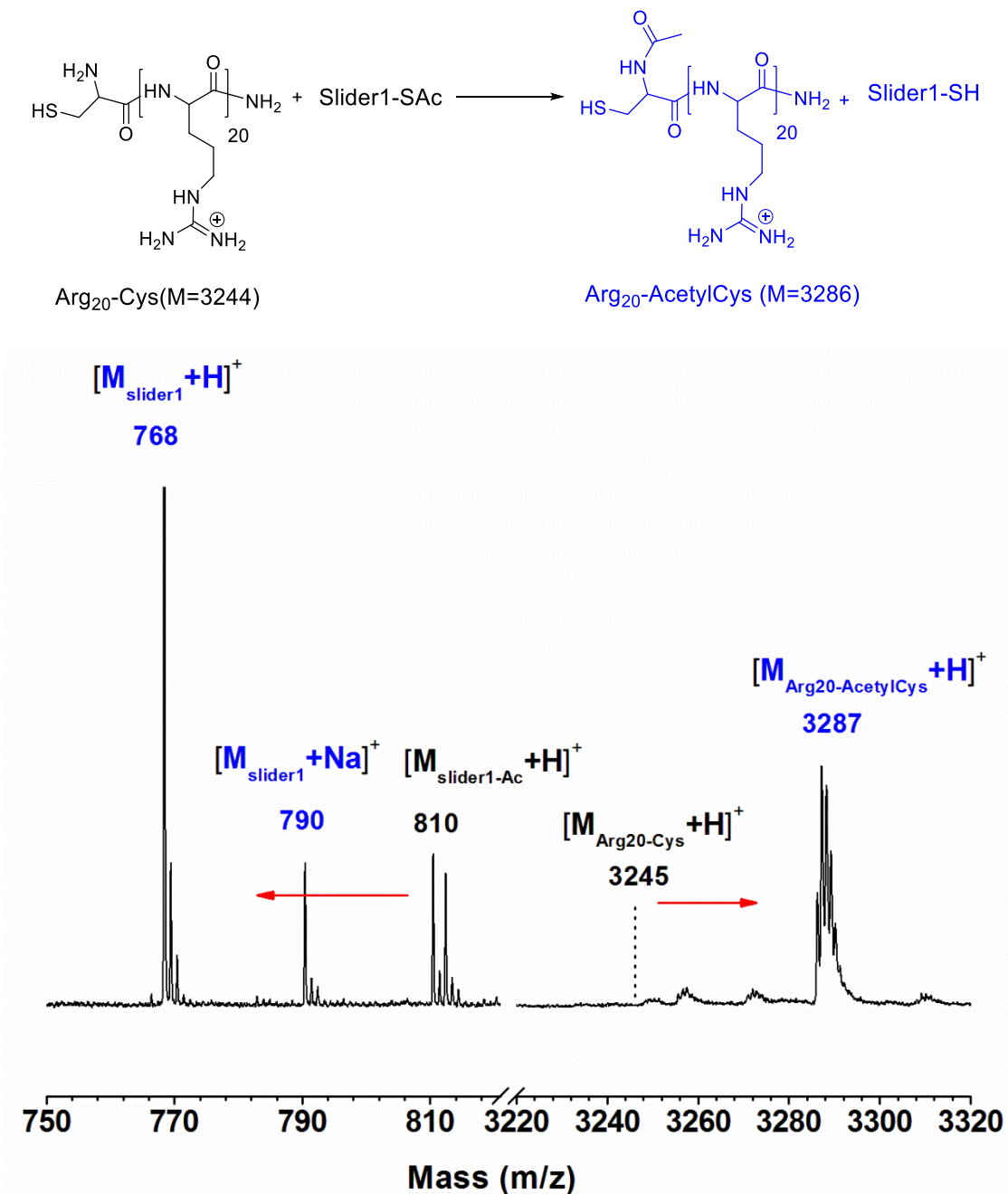
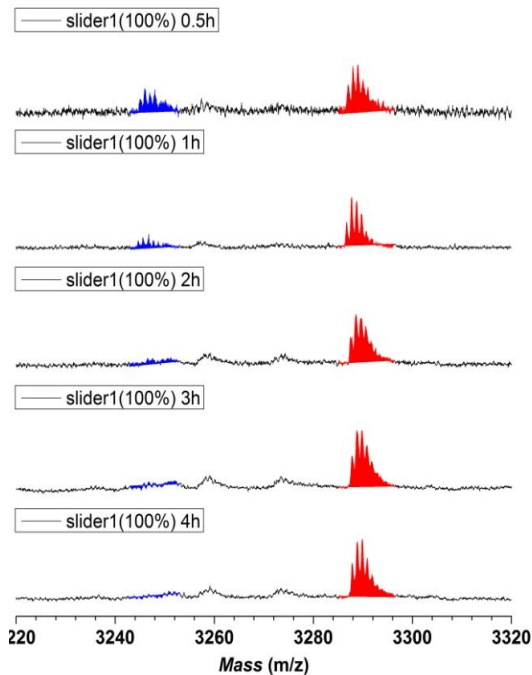


**Figure 43.** MALDI-TOF mass spectra of the reaction mixture of slider **1-SAc** (10  $\mu$ M) and Arg<sub>20</sub>-Cys (10  $\mu$ M) in MOPS buffer (10 mM, pH 7.1) after 1h. New peaks corresponding to slider **1-SH** and Arg<sub>20</sub>-AcetylCys were marked in blue.

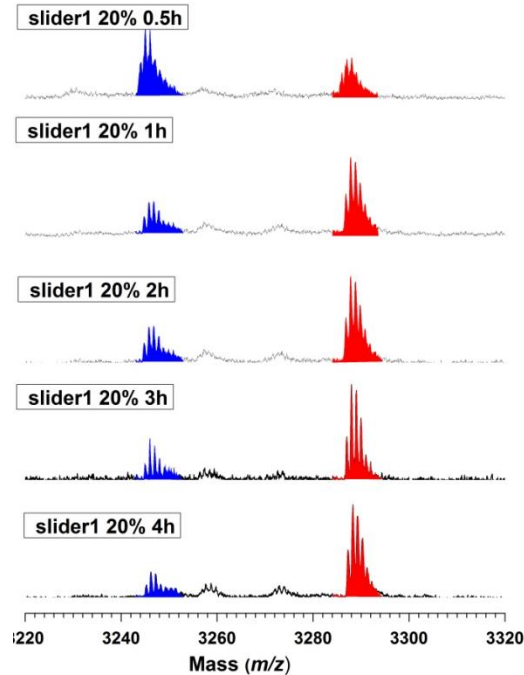
### 5.4. Standard procedure and MALDI-TOF MS analysis for acetyl transfer reactions

To a mixture of Arg<sub>18</sub>-S-Acetyl / Arg<sub>18</sub>-S-Alkyne (10 μM) and Arg<sub>20</sub>-Cys (5 μM) or Arg<sub>3</sub>-S-Acetyl (10 μM), Arg<sub>4</sub>-Cys (5 μM) and Arg<sub>5</sub> (46 μM) and Tris(3-hydroxypropyl)phosphine (THPP, 200 μM) in MOPS buffer (10 mM, pH 7.1), a certain aliquot of a stock solution of slider (final concentrations varied from 0.25 μM to 5 μM) in water was added and the mixture was shaken on a Thermo-Shaker at 25°C. At each time point, 2 μL of the reaction mixture was subjected to MALDI-TOF MS analysis.

**A**



**B**



**C**

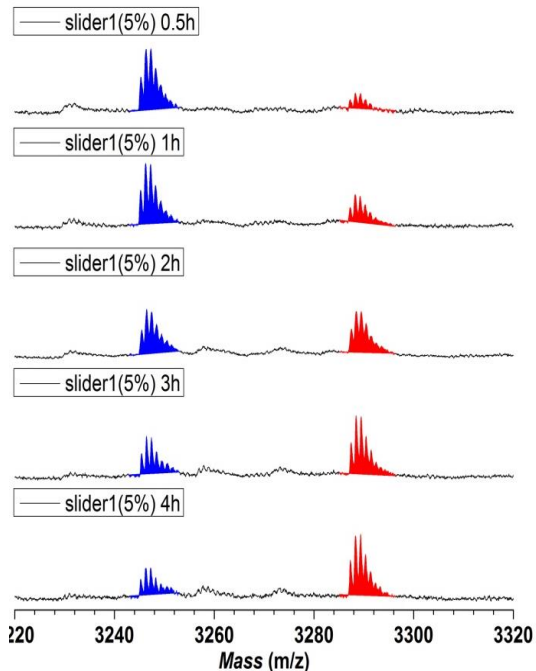


**Figure 44.** MALDI-TOF mass spectra of the acetyl transfer mixtures mediated by A) 5  $\mu\text{M}$ ; B) 1  $\mu\text{M}$ ; and C) 0.25  $\mu\text{M}$  of slider 1 at 0.5, 1, 2, 3 and 4h.

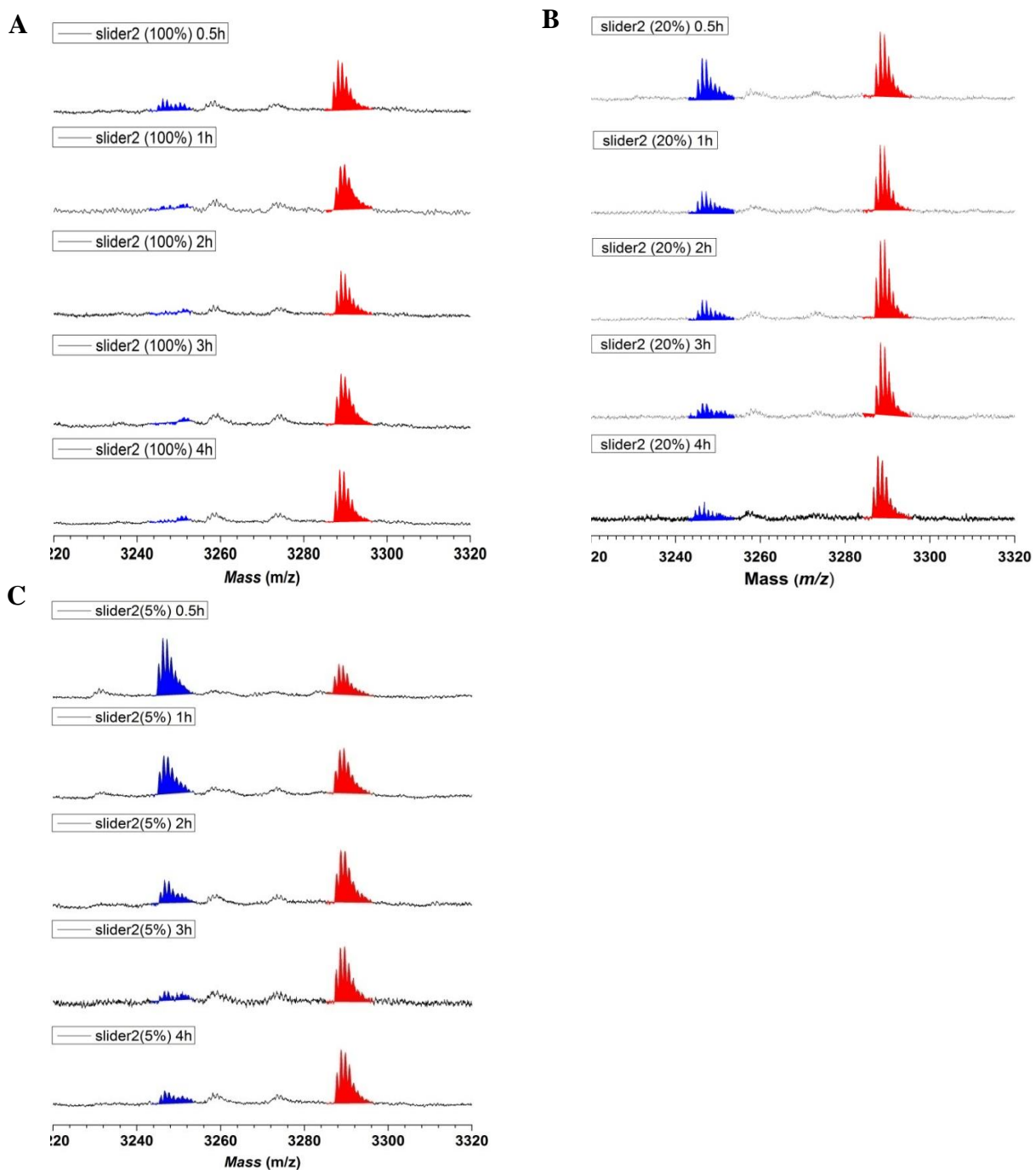


**Figure 45.** MALDI-TOF mass spectra of the acetyl transfer mixtures mediated by A) 5  $\mu\text{M}$ ; B) 1  $\mu\text{M}$ ; and C) 0.25  $\mu\text{M}$  of Slider2 at 0.5, 1, 2, 3 and 4h.

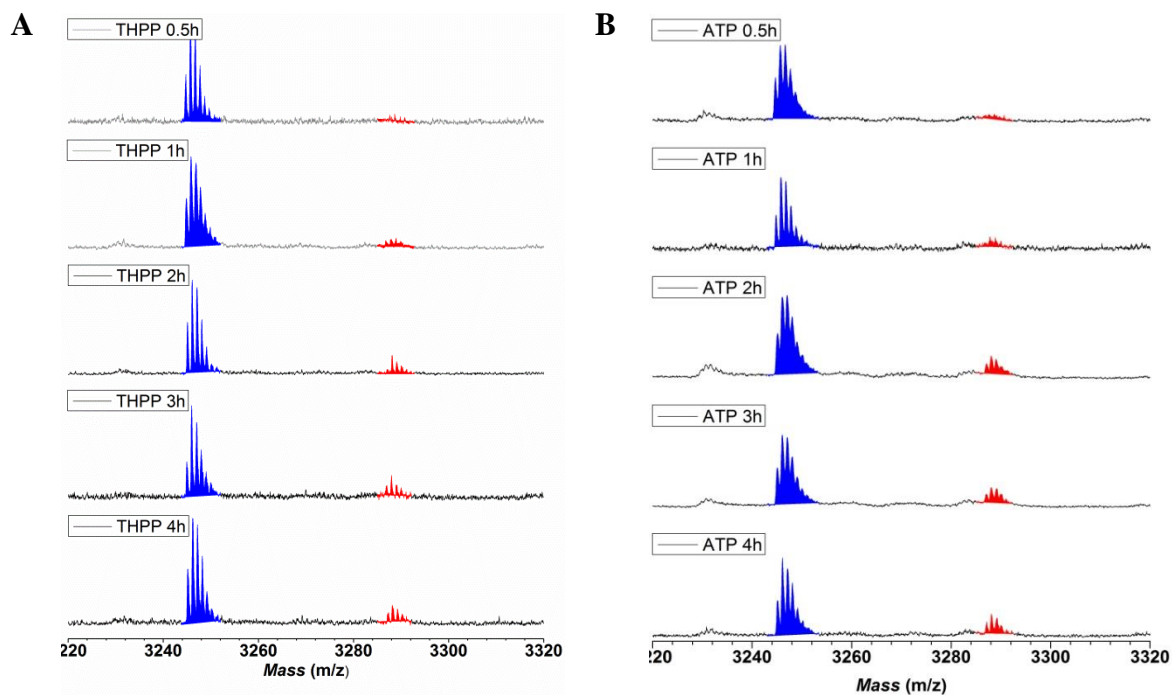


**Figure 46.** MALDI-TOF mass spectra of the acetyl transfer mixtures mediated by A) none; B) 0.25  $\mu\text{M}$  of ATP at 0.5, 1, 2, 3 and 4h.

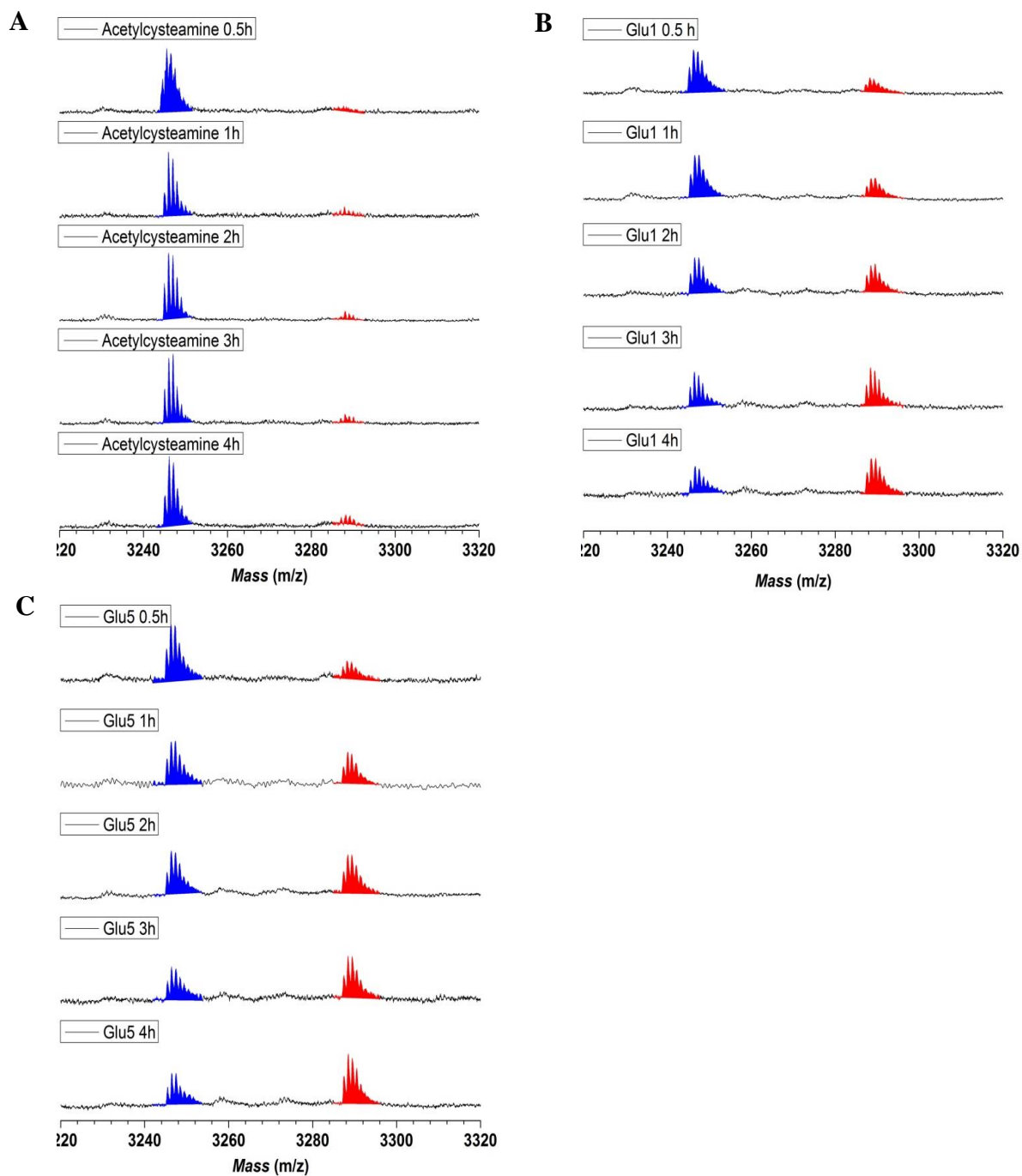


**Figure 47.** MALDI-TOF mass spectra of the acetyl transfer mixtures mediated by A) 0.25  $\mu\text{M}$  of Acetylcysteamine; B) 0.25  $\mu\text{M}$  of Glu1; C) 0.25  $\mu\text{M}$  of Glu5 at 0.5, 1, 2, 3 and 4h.



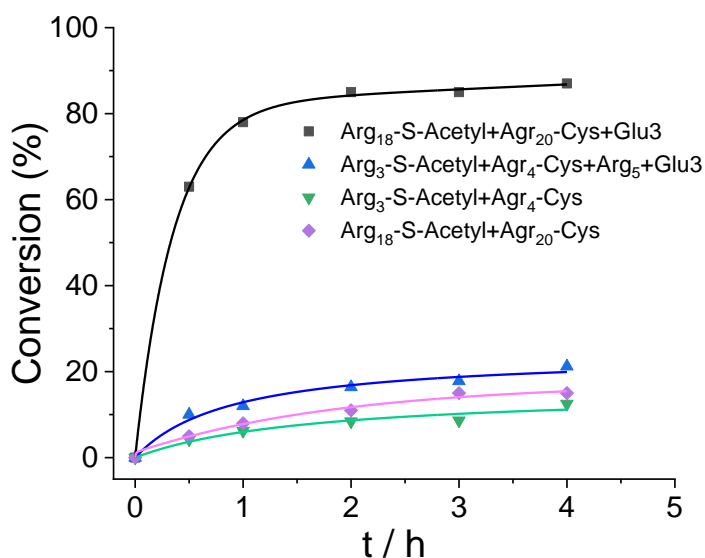


**Figure 48.** Comparison of the acetyl transfer efficiency on short (Arg<sub>3</sub>-S-Acetyl / Arg<sub>4</sub>-Cys / Arg<sub>5</sub>) and long (Arg<sub>18</sub>-S-Acetyl / Arg<sub>20</sub>-Cys) tracks.

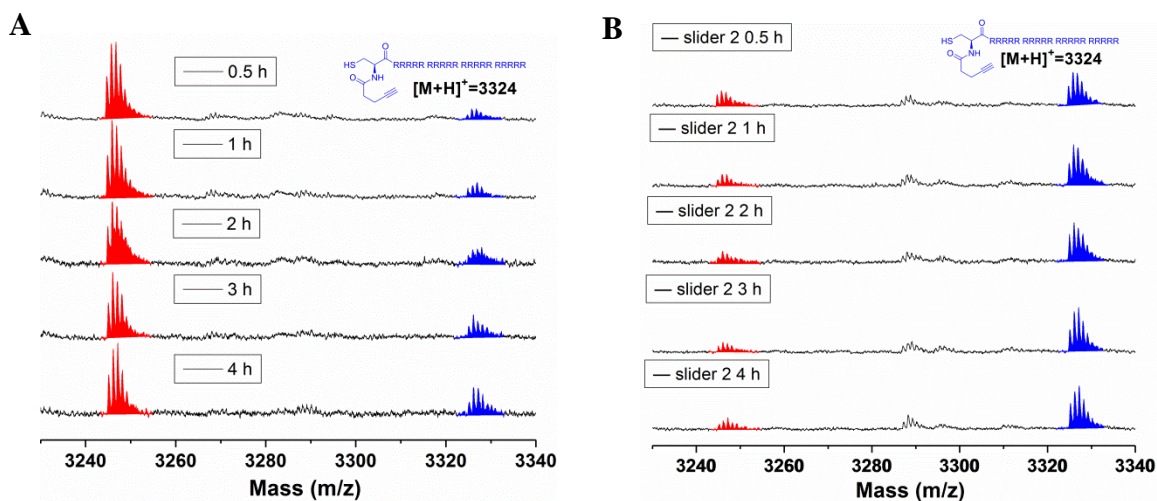


**Figure 49.** MALDI-TOF mass spectra of the alkyne transfer mixtures from Arg<sub>18</sub>-S-Alkyne to Agr<sub>20</sub>-Cys mediated by A) none; B) 0.25 μM of slider **2** at 0.5, 1, 2, 3 and 4h.

### 5.5. Post-functionalization of alkyne containing acceptor track in-situ

3-Azido-7-hydroxycoumarin was synthesized according to the reported procedure<sup>15</sup>: 2.76 g of 2,4-dihydroxy benzaldehyde, 2.34 g N-acetylglycine and 4.9 g of anhydrous sodium acetate were refluxed in 100 ml acetic anhydride for 4 h. The reaction mixture was poured onto ice to give a yellow precipitate. The obtained yellow solid was washed by ice water and then it was refluxed in a solution of conc. HCl and ethanol (2:1, 30 mL) for 1 hour, then 40 mL ice water was added to



dilute the solution. The solution was then cooled in an ice bath and  $\text{NaNO}_2$  (2.7 g) was added. The mixture was stirred for 5-10 minutes and  $\text{NaN}_3$  (3.9) was added in portions. After stirring for another 15 minutes, the filtered precipitate was washed with water, and dried under reduced pressure (0.8 g, 18% overall yield). The product was used without further purifications.  $^1\text{H}$  NMR (400 MHz, DMSO- $d_6$ ) 10.53 (s, 1 H), 7.60 (s, 1 H), 7.47 (d,  $J = 8.5$  Hz, 1 H), 6.79 (dd,  $J = 8.4, 2.2$  Hz, 1 H), 6.74 (d,  $J = 2.2$  Hz, 1 H),

100  $\mu\text{L}$  alkyne transfer mixture of Arg $_{18}$ -S-Alkyne (100  $\mu\text{M}$ ), Arg $_{20}$ -Cys (50  $\mu\text{M}$ ), slider 2 (10  $\mu\text{M}$ ) and Tris(3-hydroxypropyl)phosphine (THPP, 200  $\mu\text{M}$ ) in MOPS buffer (10 mM, pH 7.1) was allowed to react for 4h. To this solution, another 100  $\mu\text{L}$  DMSO solution containing 3-azido-7-hydroxycoumarin (200  $\mu\text{M}$ ),  $\text{CuSO}_4$  (1.6 mM) and sodium ascorbate (1.6 mM) was added. The mixture was shaken on a Thermo-Shaker at 25 $^\circ\text{C}$  for overnight. Afterwards the small molecules were removed by using a centrifugal filter and then the rest of the reaction mixture was subjected to MALDI-TOF MS analysis.

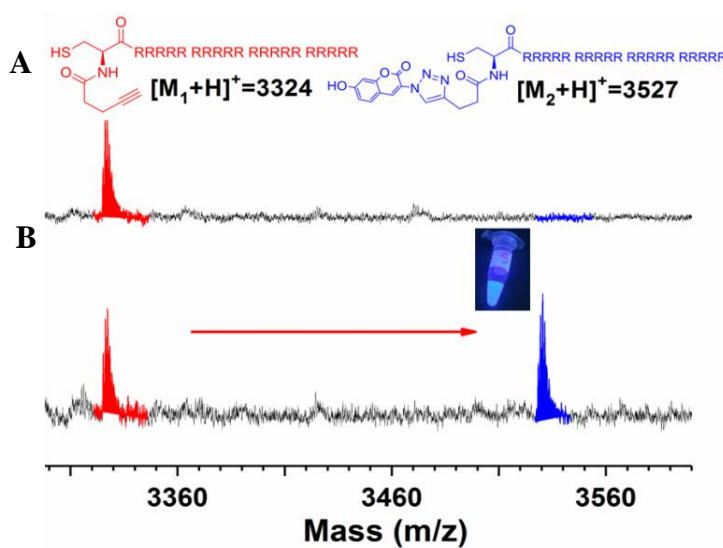


**Figure 50.** MALDI-TOF mass spectra of the alkyne transfer mixtures A) before click reaction; B) after click reaction; fluorescent image was taken under 365 nm UV light lamp.

## 6. Molecular cargo transport within physically separated compartments

### 6.1. Preparation of nc-PAAm and agarose hydrogels

Negatively charged polyacrylamide hydrogels were prepared according to a standard procedure. Prepolymer solution containing acrylamide (20%), acrylic acid (0.4%), bis-acrylamide (0.4%) and required amounts of 2,2'-Azobis(2-methylpropanitrile) as photo-initiator was casted between two glass slides separated by a thin spacer (ca. 0.2 mm). Polymerization was initiated by irradiation under a 365 nm UV lamp. Agarose hydrogels were prepared from a hot 2% w/w solution of agarose

casted using the same set-up. After gelation, all the gel layers were gently peeled off and stored in 10 mM MOPS buffer (pH 7.1).

## 6.2. Synthesis of Arg18-S-Coumarin and its diffusion inside nc-PAAm gel matrix

The synthesis of Arg18-S-Coumarin was following the procedure for Arg<sub>18</sub>-S-Acetyl using a commercially available Coumarin 343 X NHS ester (Lumiprobe; Excitation maximum:437 nm; Emission maximum: 477 nm).

The diffusion of Arg18-S-Coumarin inside nc-PAAm gel matrix was studied microscopically. Two pieces of nc-PAAm gels were soaked in 10mM MOPS buffer (pH 7.1) containing 200  $\mu$ M Arg20, while another piece of nc-PAAm gel was soaked with 200  $\mu$ M Arg18-S-Coumarin in the same buffer for 8 h. Then a tri-layer system consisting these gels was constructed with Arg18-S-Coumarin in the central layer. The obtained construct was placed on the microscope stage. The diffusion of Arg18-S-Coumarin into either top or bottom gel was recorded over a time periods of 2 h (Movie 1). It shows that Arg<sub>18</sub>-S-Coumarin does not significantly diffuse into other two layers for at least 2 h.

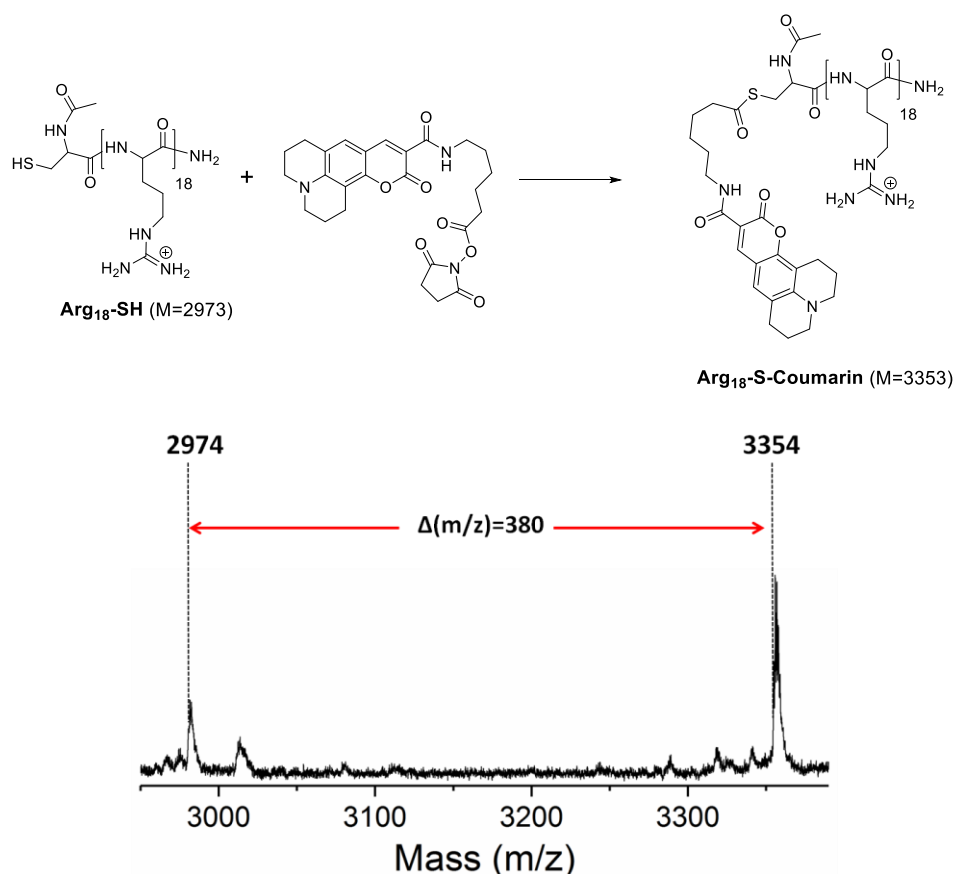


**Figure 51.** MALDI-TOF mass spectra of Arg18-S-Coumarin.

## 6.3. Diffusion of CoA-NBD inside the gel matrix by wet stamping

In a 20mL glass bottle, 4-Chloro-7-nitrobenzofurazan (NBD) (140 mg; 0.7 mmol) was dissolved in 2 mL of DMF. Coenzyme A (10 mg; 0.013 mmol) was dissolved in 1 ml of DMF/water (vol/vol=9/1). The CoA solution was added dropwise into the reaction mixture. The reaction mixture was stirred for overnight at room temperature under Argon. The solvent were removed by flushing with N<sub>2</sub>, and the crude product was dissolved in water and washed with E<sub>2</sub>O and CH<sub>2</sub>Cl<sub>2</sub>. The final product was obtained after freeze-drying. Isolated yield = 90%. <sup>1</sup>H NMR (400MHz, D<sub>2</sub>O): 8.50 (1H, s), 8.38 (1H, d), 8.22 (1H, s), 7.27 (1H, d), 5.95 (1H, d), 4.47 (1H, s), 4.13 (2H, s), 3.87 (1H, s), 3.73 (1H, m), 3.37 (7H, m), 2.27 (2H, t), 0.78 (3H, s), 0.65 (3H, s).

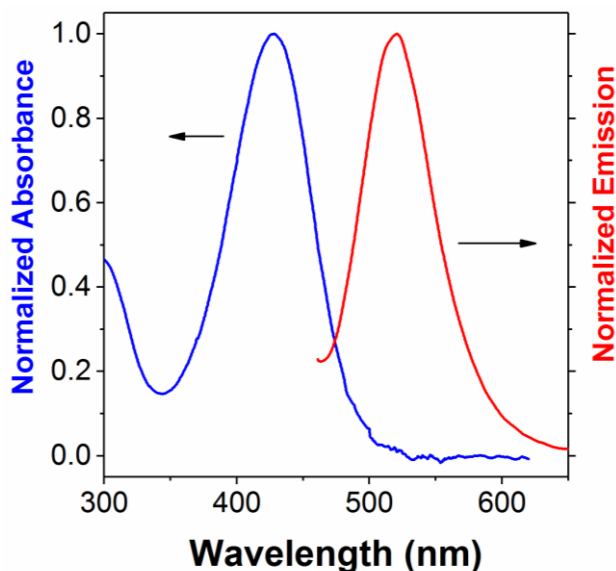
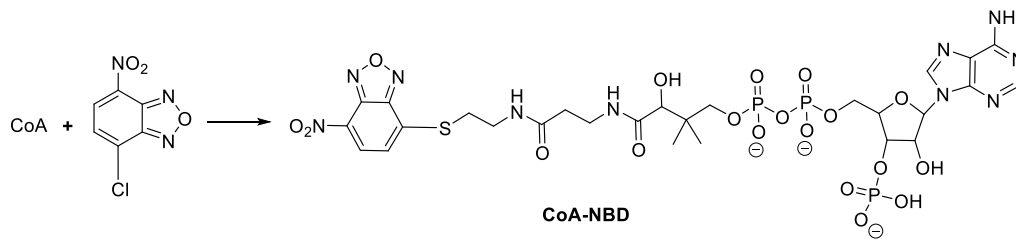


**Figure 52.** Absorption and emission spectra of CoA-NBD (0.1 mM in H<sub>2</sub>O), measurements were normalized to the highest intensity. Absorption maximum: 423 nm; Emission maximum: 523 nm.

The modified wet stamping procedure is as following: Two pieces of nc-PAAm gels were soaked in 10mM MOPS buffer (pH 7.1) containing 200 μM Arg20 equilibrated in solution for 8h. A 2% agarose stamp was soaked in a CoA-NBD solution (100 μM) for 4 h. Then the nc-PAAm gels were dried for 30 s and placed in the petridish containing a piece of wet cotton to prevent drying during an experiment. The agarose stamp was brought in contact (feature side down) with the nc-PAAm gel. The obtained construct was placed on the microscope stage. The contact of the stamp pillars with the nc-PAAm gel was brought into focus and a series of fluorescent images were acquired.

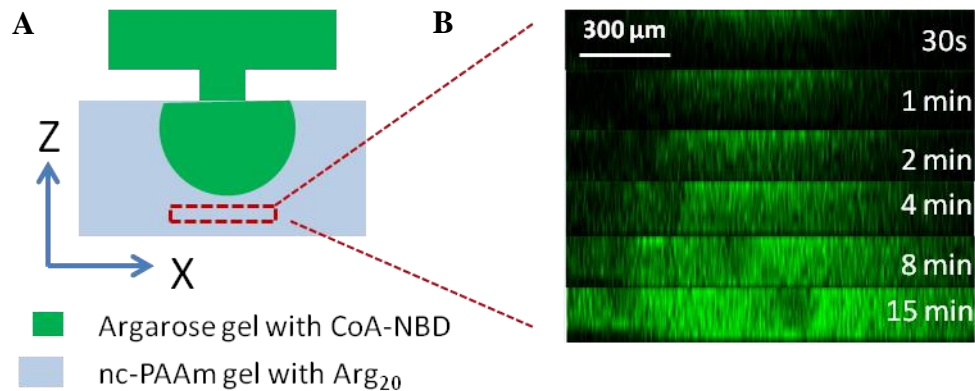


**Figure 53.** A) Schematic description of the diffusive spreading of CoA-NBD from an agarose stamp (2%) with 250 μm wide microfabricated pillars into nc-PAAm hydrogels containing positively charged Arg<sub>20</sub> tracks and B) the vertical cross sections (XZ) from each experimental micrograph of the bottom gel at different time points.

#### 6.4. Test of chemical reactivity in different hydrogels

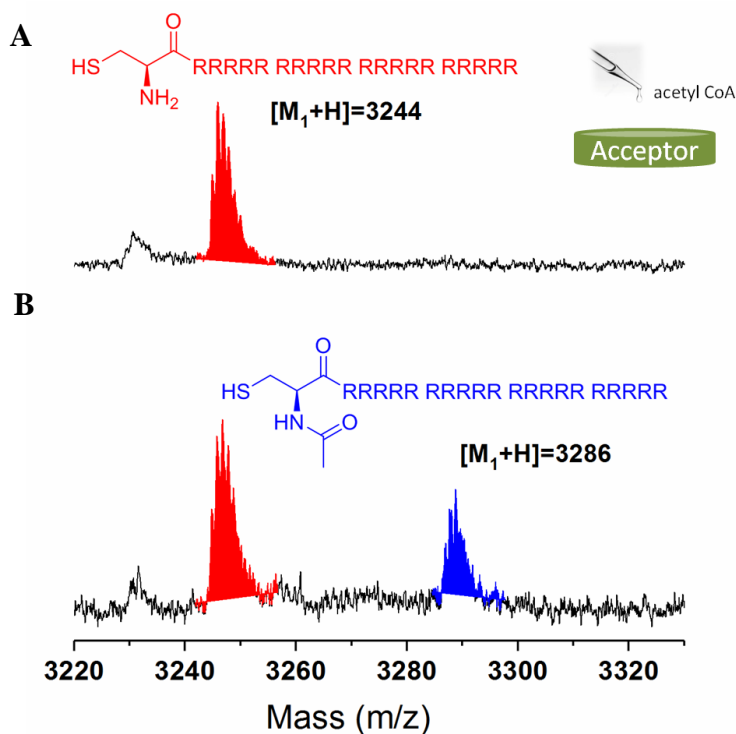


**Figure 54.** MALDI-TOF mass spectra of acetyl CoA reaction with Arg<sub>20</sub>-Cys in A) nc-PAAm gel and B) agarose gel after 1 h.

## 7. References

1. Priftis, D.; Laugel, N.; Tirrell, M. *Langmuir* **2012**, *28*, 15947–15957.
2. Phillips, J. C.; Braun, R.; Wang, W.; Gumbart, J.; Tajkhorshid, E.; Villa, E.; Chipot, C.; Skell, R. D.; Kale, L.; Schulten, K. *J. Comput. Chem.* **2005**, *26*, 1781-1802.
3. Vanommeslaeghe, K.; Hatcher, E.; Acharya, C.; Kundu, S.; Zhong, S.; Shim, J.; Darian, E.; Guvench, O.; Lopes, P.; Vorobyov, I.; Mackerell, A. D. J. *J. Comput. Chem.* **2010**, *31*, 671-690.
4. Vanommeslaeghe, K.; Raman, E. P.; MacKerell Jr, A. D. *J. Chem. Inf. Model.* **2012**, *52*, 3155-3168.
5. Frisch, M. J.; Trucks, G. W.; Schlegel, H. B. Gaussian, Inc., Wallingford, CT **2009**, 1.
6. Mayne, C. G.; Saam, J.; Schulten, K.; Tajkhorshid, E.; Gumbart, J. C. *J. Comput. Chem.* **2013**, *34*, 2757-2770.
7. Humphrey, W.; Dalke, A.; Schulten, K. *J. Molec. Graphics* **1996**, *14*, 33-38.
8. MacKerell Jr, A. D.; Bashford, D.; Bellott, M.; Dunbrack Jr., R. L.; Evanseck, J. D.; Field, M. J.; Fischer, S.; Gao, J.; Guo, H.; Ha, S.; Joseph-McCarthy, D.; Kuchnir, L.; Kuczera, K.; Lau, F. T. K.; Mattos, C.; Michnick, S.; Ngo, T.; Nguyen, D. T.; Prodhom, B.; Reiher, I. *J. Phys. Chem. B* **1998**, *102*, 3586-3616.
9. MacKerell Jr, A. D.; Feig, M.; Brooks, C. L. *J. Comput. Chem.* **2004**, *25*, 1400-1415.
10. Darden, T.; York, D.; Pedersen, L. *J. Chem. Phys.* **1993**, *98*, 10089-10092.
11. Giorgino, T. Computing diffusion coefficients in macromolecular simulations: the Diffusion Coefficient Tool for VMD, Submitted (**2015**), Available from GitHub.
12. Fiorin, G.; Klein, M. L.; Hémin, J. *Mol. Phys.* **2013**, *111*, 3345-3362.
13. Grossfield, A. *University of Rochester Medical Center: Rochester, NY, accessed April 2017.* **2012**.
14. Kumar, S.; Rosenberg, J. M.; Bouzida, D.; Swendsen, R. H.; Kollman, P. A. *J. Comput. Chem.* **1992**, *13*, 1011-1021.
15. Sivakumar, K.; Xie, F.; Cash, B. M.; Long, S.; Barnhill, H. N.; Wang, Q. *Org. Lett.*, **2004**, *6*, 4603-4606.